Texas A&M
Transportation
Institute

Application of Superpave Gyratory Compactors for Flexible Base and Subgrade

Technical Report 0-6883-R1

Cooperative Research Program

1. Report No. FHWA/TX-17/0-6883-R1	2. Government Accession No.	3. Recipient's Catalog No.
4. Title and Subtitle APPLICATION OF SUPERPAVE GYRATORY COMPACTORS FOR FLEXIBLE BASE AND SUBGRADE		5. Report Date Published: January 2019
		6. Performing Organization Code
7. Author(s) Sang Ick Lee, Stephen Sebesta, Poura Arabali, Robert Lytton, and Maryam Sakhaeifar		8. Performing Organization Report No. Report 0-6883-R1
9. Performing Organization Name and Address Texas A&M Transportation Institute College Station, Texas 77843-3135		10. Work Unit No. (TRAIS)
		11. Contract or Grant No. Project 0-6883
12. Sponsoring Agency Name and Address Texas Department of Transportation Research and Technology Implementation Office 125 E 11th Street Austin, Texas 78701-2483		13. Type of Report and Period Covered Technical Report: September 2015–August 2017
		14. Sponsoring Agency Code

16. Abstract
The impact hammer compaction has historically been used to develop moisture-density curves and fabricate specimens for strength testing for flexible base and subgrade materials. However, the precision of compressive strength results by the impact hammer compaction remains a concern that can result in conflicting test results on whether a material meets specification requirements. This project used the Superpave Gyratory Compactor (SGC) to analyze if SGC compaction enables improved precision of compressive strength tests for flexible base and subgrade materials and analyzed a procedure for determining the moisture-density curve of base and subgrade materials using the SGC. Also, the applicability of SGC for base materials was evaluated in context of mechanistic-empirical (M-E) pavement design methods. The results showed that SGC compaction produced compressive strength results with less variability and improved precision compared to impact hammer compaction. Also, from the measurement of M-E properties, base materials compacted with the SGC were associated with lower permanent strain and higher resilient modulus than the materials with the impact hammer. The evaluation of internal structure using X-ray Compute Tomography and Aggregate Image Measurement System helped explain the behavior of materials compacted with both impact hammer and SGC compaction methods.

17. Key Words Superpave Gyratory Compactor, SGC, Impact Hammer Compaction, Compressive Strength Test, Base, Subgrade, Flexible Base, Proctor Compaction, Tex-113-E, Tex-114-E, Aggregate Imaging, AIMS		18. Distribution Statement No restrictions. This document is available to the public through NTIS: National Technical Information Service Alexandria, Virginia 22312 http://www.ntis.gov	
19. Security Classif. (of this report) Unclassified	20. Security Classif. (of this page) Unclassified	21. No. of Pages 74	22. Price

APPLICATION OF SUPERPAVE GYRATORY COMPACTORS FOR FLEXIBLE BASE AND SUBGRADE

by

Sang Ick Lee
Assistant Research Engineer
Texas A&M Transportation Institute

Stephen Sebesta
Research Scientist
Texas A&M Transportation Institute

Poura Arabali
Graduate Research Assistant
Texas A&M Transportation Institute

Robert Lytton
Research Engineer
Texas A&M Transportation Institute

and

Maryam Sakhaeifar
Assistant Research Engineer
Texas A&M Transportation Institute

Report 0-6883-R1
Project 0-6883
Project Title: Compaction of Soils and Base Materials using Superpave Gyratory Compactors

Published: January 2019

TEXAS A&M TRANSPORTATION INSTITUTE
College Station, Texas 77843-3135

DISCLAIMER

This research was performed in cooperation with the Texas Department of Transportation (TxDOT) and the Federal Highway Administration (FHWA). The contents of this report reflect the views of the authors, who are responsible for the facts and the accuracy of the data presented herein. The contents do not necessarily reflect the official view or policies of the FHWA or TxDOT. This report does not constitute a standard, specification, or regulation.

This report is not intended for construction, bidding, or permit purposes. The researcher in charge of the project was Stephen Sebesta.

The United States Government and the State of Texas do not endorse products or manufacturers. Trade or manufacturers' names appear herein solely because they are considered essential to the object of this report.

ACKNOWLEDGMENTS

TABLE OF CONTENTS

LIST OF FIGURES

Page

LIST OF TABLES

Page

CHAPTER 1. LITERATURE REVIEW

OVERVIEW

To begin this project, researchers determined the current state of the practice and emerging research using the Superpave gyratory compactor (SGC) for base and subgrade materials, and then select the most promising SGC equipment of use in this project, with a focus on the following activities:

- Conduct a literature review related to using SGC for soil and base materials via scientific and research publications.
- Search domestic and international SGC equipment and contact each equipment manufacturer to determine the capabilities of their current suit of SGCs.
- Determine the equipment most suitable for meeting the test factorial requirements of the project

REVIEW OF RELEVANT WORKS USING SGC FOR SOILS AND BASE MATERIALS

Minnesota Department of Transportation

Minnesota Department of Transportation (MnDOT) conducted the resilient modulus tests on 20 samples of base course materials, which contained various fractions of recycled asphalt pavement materials and aggregates to investigate the effect of recycled asphalt pavement materials and moisture content on the resilient modulus values (*1*). As a part of this study, the test specimens were compacted with gyratory compaction since it was questionable that Proctor compaction can simulate the field compaction and material moisture can escape from the mold in Proctor compaction. The maximum dry densities (MDD) and optimum moisture contents (OMCs) obtained from both gyratory and Proctor compactions were compared. The density from gyratory compaction was closer to the field density. The following compaction parameters were used to mold test specimens by the gyratory compaction:

- Specimen diameter: 6 in.
- Gyration rate: 30 gyration/min.
- Gyration angle: 1.25°.
- Compaction pressure: 600 kPa.

The comparison of resilient modulus test results, field density, and moisture content of specimens compacted with 50 and 75 gyrations, led to the selection of 50 gyrations for this study. Figure 1 shows the gyratory compactor used in this study and a representative specimen compacted by the gyratory compactor after strength testing.

(a) Gyratory compactor.   **(b) Specimen after strength test.**

Figure 1. MnDOT Gyratory Compactor and Specimen Compacted (*1*).

U.S. Army Corps of Engineers

U.S. Army Corps of Engineers conducted gyratory compaction tests on crushed limestone to investigate the effect of vertical pressure, gyration angle, and number of gyrations (*2*). This research effort investigated gyratory compaction as a potential laboratory compaction method that can produce desirable densities close to ones in the field under traffic loading. The moisture-density curves developed from impact and gyratory compactions were compared. California Bearing Ratio, an index representative of shear stress, sample rebound after gyrations, reproducibility of gyration compaction results, and aggregate degradation after compaction were also investigated. The following parameters were set for the gyratory compaction:

- Specimen diameter: 6 in.
- Gyration angle: 1 and 2°.
- Compaction pressure: 25, 50, 100, 150, and 200 psi.
- Number of gyration: 30 and 120.

One of the test variables was kept constant while the other two parameters were varied to investigate the effect of each parameter. Moisture-density relationships from the gyratory compaction were similar to those from the impact compaction method, but gyratory compaction showed greater densities at lower water content. Increasing the compaction pressure produced greater increases in density than increasing either of the gyration angle or number of revolutions. Furthermore, the aggregate test results before and after gyratory compaction showed that a minimum of aggregate degradation occurred.

Montana State University

Montana State University conducted a feasibility study for SGC application for soil compaction and evaluated different compaction parameters that affect compaction efforts (*3*). The motivation of this study was that while only impact loading is used for soil compaction in Proctor testing in the laboratory, a combination of kneading, vibration, and normal pressure effects contribute to

2

field compaction, and there might be a better method to simulate field compaction in the laboratory. For this purpose, the comparison between dry densities obtained from the SGC and the Proctor methods was made using four types of soils to cover a wide range of American Association of State Highway and Transportation Officials (AASHTO) soils classification, including: A-1-a (stone fragments, gravel, and sand), A-3 (fine non-plastic sand), A-4 (silt), and A-7-6 (clay). An AFGC125X gyratory compactor from Pine Instrument Company was used for all gyratory compaction tests conducted in this study. While the gyration angle and rate were fixed at 1.25° and 30 gyrations per minute, respectively, only two parameters were explored for effective gyratory compaction as:

- Number of gyrations: up to 500 gyrations at desired contact pressure with recording sample height for each gyration.
- Contact pressure: 200, 300, 400, 500, and 600 kPa for dry samples and 200 and 600 kPa for wet samples.

The study demonstrated that increasing the contact pressure is the most effective method to increase density of fine-grained soils while increasing the number of gyrations is effective for non-cohesive, granular soils. However, the densities from SGC were not substantially different than ones from traditional laboratory Proctor method, even though the physical process of achieving compaction is quite different. Furthermore, the study found a potential issue to be solved that water might be exuded through gaps around the perimeter of the top or bottom plates of the gyratory mold, especially for granular free-draining soils compacted at higher water contents as illustrated in Figure 2.
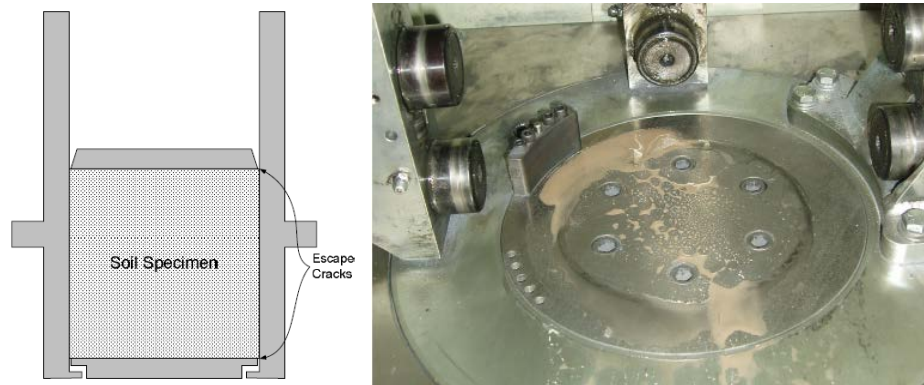
(a) Locations of Water Escape   (b) Accumulated water in the bottom of SGC

Figure 2. Water Escape from the SGC Mold.

Florida Department of Transportation

The Florida Department of Transportation conducted an experimental study using two sandy subgrade soils to evaluate how laboratory compaction methods can simulate field compaction techniques (*4*). The IPC Servopac gyratory compactor was used for all gyratory compaction tests in this study. The following parameters were set as:

- Compaction pressure: 100 to 500 kPa.
- Gyration angle: 1.0 and 1.25°.

- Gyration rate: 20 gyrations per min.
- Number of gyrations: 30, 60, and 90.

This study found that the compaction pressure as a way of increasing the dry density was not very effective when the pressure was higher than 200 kPa. This effect was similar to what was experienced during the laboratory impact compaction tests of the soils, which showed that increasing the hammer weight did not increase the dry density during the impact compaction. On the other hand, the number of gyration had a significant effect on the densities of the two soils, that is, the dry densities increased with increasing number of gyrations. The gyratory parameters with 200 kPa pressure, 1.25° gyration angle, 90 gyrations, and 20 gyrations per minute showed considerable promise for replicating field compaction characteristics.

REVIEW OF RELEVANT WORKS ON UPCOMING TASKS

Characteristics of base course materials play an important role in the pavement design. One of the factors for base course characterization in mechanistic-empirical (M-E) pavement design is resilient modulus. For instance, Hossein and Lane tested 16 different materials from Virginia for developing a catalogue for resilient modulus to be used in M-E pavement design for Virginia Department of Transportation (5). They developed a range of resilient modulus for different rock types from different sources for use as reference values in M-E design.

The internal aggregate structure of asphalt concrete after compaction plays an important role in performance characteristics of this material, and this structure is required to be adequately quantified (6). Aggregate interlock or point to point contact between aggregates, aggregates orientation, and spatial distribution of aggregates after compaction influence the physical performance of asphalt concrete, and different field and laboratory compaction methods can cause differences in these parameters.

Evaluation of internal structure of aggregates can be performed by obtaining digital images of this structure after compaction. Digital image techniques in combination with quantification of aggregate structure characteristics can be used for quality control and assurance purposes (6). They used some digital image processing and analysis methods to quantify the internal aggregate structure of asphalt concrete. These input data about asphalt mixtures have been used for calibration of image filtering parameters. This analysis can help compute the number of contact points between aggregates, and determine radial distribution and aggregate orientation, and segregation of aggregates. Furthermore, by using gyratory compaction, the effects of compaction parameters, such as compaction pressure, aggregate type, nominal maximum aggregate size, and temperature on internal aggregate structure measurements were studied.

Some studies have used the X-ray imaging system to investigate the air void distribution in the asphalt concrete mixtures. The assessment of X-ray images of asphalt concrete mixtures by Dehghan et al. showed that the size and shape of air voids in asphalt mixtures are dependent on the aggregates structure around them (7). X-ray tomographic imaging is the best way for studying the air voids in the mixture; however, numerical methods may be able to replace the expensive X-ray method for generating the air void distributions.

SUPERPAVE GYRATORY COMPACTORS FOR THE PROJECT

Researchers explored various SGC to determine the equipment most suitable for meeting the test factorial requirements of this project. The effort was performed through searching the operator manuals and/or specifications and contacting the equipment manufacturers to collect the technical capabilities of each SGC. Table 1 lists the SGC equipment and the technical specification and operating parameters of each compactor. Based on comparing the SGCs and discussion with the Texas Department of Transportation (TxDOT), researchers selected the Pine AFG2 compactor.

Table 1. Gyratory Compactors for Base and Subgrade Material Compaction.

	Manufacturer	Troxler	IPC Global		Pine Test Equipment		Humboldt	Controls (PAVELAB Gyrocomp)	
	Model	5850	SERVOPAC	GYROPAC	AFG2	AFGB1	AFGB	Standard	Research
Compaction Parameter	Contact Pressure (kPa)	90 to 1,000	10 to 999	0 to 700	200 to 1,000	300 to 630	300 to 1,000	- 80 to 800 for 150 mm Dia. - 160 to 1400 for 100 mm Dia.	- 80 to 800 for 150 mm Dia. - 160 to 1400 for 100 mm Dia.
	Gyration angle (°)	0 to 1.5 (int. & ext.)	0 to 3	0 to 3	0 to 1.5 (int. & ext.)	- 0.82 or 1.16 int. - 1.25 ext.	- 0.82 or 1.16 int. - 1.25 ext.	0.70 to 1.40 (internal)	0 to 3 (internal)
	Gyration rate (gyr./min.)	30	3 to 60	60	30	20 to 40	30	15 to 60	15 to 60
	No. of Gyrations	1 to 999	1 to 999	N/A*	0 to 999	0 to 299	0 to 299	0 to 999	0 to 512
Sample Size (mm)	Diameter	100 or 150	100 or 150	100 or 150	100 or 150	150	150	100 or 150	100 or 150
	Height	50 to 317.5	50 to 170	- 65 for 100 mm Dia. - 85 for 150 mm Dia.	Up to 210	10 to 200	10 to 215	- 50 to 125 for 100 mm Dia. - 80 to 200 for 150 mm Dia.	- 50 to 150 for 100 mm Dia. - 80 to 240 for 150 mm Dia.
	Compaction Mode	- No. of gyration - Sample height	- No. of gyration - Sample height	- Sample height	- No. of gyration - Sample height	- No. of gyration - Sample height	- No. of gyration - Sample height	- No. of gyration - Sample height	- No. of gyration - Sample height
	Adjusting Compaction Parameters in	Control panel	Computer	Computer	Control panel	Control panel	Control panel	Computer	Computer
	Pressure Operation	Electro-Hydraulic	Pneumatic	Electro-pneumatic	Electro-mechanical	Hyd. & elector-mechanical	Hyd. & elector-mechanical	Pneumatic	Pneumatic
	Standard	AASHTO T312, ASTM D6925	AASHTO T312, ASTM D6925	Australian Standard	AASHTO T312, ASTM D6925	AASHTO T312, ASTM D6925	AASHTO T312, ASTM D6925	AASHTO T312, ASTM D6925	AASHTO T312, ASTM D6925
	Price (w/ calibration kit)	$41,950	$46,821	-	$39,331	$33,460	$31,129	$30,150	$39,343
Suitability on Project**	Contact Pressure	O	O	Δ	O	Δ	O	O	O
	Gyration angle	Δ	O	O	Δ	× (fixed)	× (fixed)	Δ	O
	Gyration rate	× (fixed)	O	× (fixed)	× (fixed)	O	× (fixed)	O	O
	Sample diameter (Base/subgrade)	O/O	O/O	O/O	O/O	O/×	O/×	O/O	O/O
	Sample height. (Base/subgrade)	O/O	×/O	×/×	O/O	×/O	O/O	×/O	O/O

* Allows specimens to be compacted to a predetermined height

** O: applicable, Δ: applicable but limited, ×: not applicable

SUMMARY

Base on the literature review, the gyratory compaction parameters such as gyration angle, number of gyrations, rate of gyrations, and confining pressure may affect the gyratory and field compaction simulation. The effect of each parameter may vary depending on the soil types. For instance, the effect of compaction pressure and number of gyrations may differ on fine-grained soils and non-cohesive granular soils. Therefore, a comprehensive factorial analysis would be required to fully investigate the effect of these parameters on moisture-density curves, compressive strength test results, M-E pavement design input parameters, and internal structure of materials after compaction. Also, researchers evaluated various SGC machines and selected the Pine AFG2 compactor to be used in this project.

CHAPTER 2. EVALUATION OF PRECISION OF COMPRESSIVE STRENGTH

OVERVIEW

This chapter describes if compaction with the SGC improves the precision of compressive strength results as compared to compaction with the impact hammer. The evaluation was performed through the following procedure:

- Select and collect flexible base and subgrade soil materials.
- Develop a procedure to attain the applicable Tex-113-E and Tex-114-E MDD using the SGC, including compaction parameters.
- Compact materials with the impact hammer and SGC, and determine compressive strength, moisture content, and dry density.
- Statistically evaluate if the SGC compaction yields improved, equivalent, or reduced precision as compared to the impact hammer compaction.

COLLECTION OF TESTING MATERIALS

With input from TxDOT, researchers selected five flexible base materials and one subgrade soil. The flexible base materials were collected from the stockpiles or quarry located at Pharr, Waco, Atlanta, Amarillo, and San Antonio. Researchers used a high plasticity index subgrade material collected from the Paris District. Using these materials, OMC and MDD were determined based on the Tex-113-E for base and Tex-114-E for subgrade materials in the laboratory. Table 2 presents the properties of each material.

Table 2. Material Properties of Base and Subgrade Materials.

Material Properties		Base Materials					Subgrade
		Pharr	**Waco**	**Atlanta**	**Amarillo**	**San Antonio**	
Material Type/Grade	Type	Type E (Caliche)	Type D (Sandstone)	Sandstone	Type B (Gravel)	Type A (Crushed Stone)	-
	Grade	Grade 4	Grade 4	Grade 5	Grade 4	Grade 2	-
Gradation (% passing)	1 ¾ in.	100	100	100	100	100	100
	7/8 in.	89	77	93	81	97	100
	3/8 in.	76	65	56	55	51	100
	# 4	43	43	43	47	30	96
	# 40	19	25	21	23	17	32
Atterberg Limit	Liquid limit	27	20	14	-	21	52
	Plastic Index	5	5	3	-	5	33
M-D Curve	OMC (%)	12.78	8.21	6.67	5.19	6.48	20.39
	MDD (pcf)	112.62	130.95	134.30	138.63	137.47	110.29

DEVELOPMENT OF SGC COMPACTION PROCEDURE

To begin work with the SGC to compact the base and subgrade materials, researchers developed a procedure to attain the applicable Tex-113-E or Tex-114-E MDD using the SGC machine.

Specimen Sizes

Based on Tex-113 and 114-E, the test specimens should be compacted in a 6 in. diameter and 8 in. tall mold for base material and a 4 in. diameter and 6 in. tall for subgrade soil. However, since the Pine AFG2 Gyratory Compactor used for the study uses molds with 150 mm (5.91 in.) or 100 mm (3.94 in.) diameter, researchers compacted the samples in those slightly smaller molds for SGC compaction as:

- Base: 150 mm (5.91 in.) diameter × 200 mm (7.87 in.) tall.
- Subgrade: 100 mm (3.94 in.) diameter × 150 mm (5.91 in.) tall.

Both sizes of specimens compacted with the impact hammer and SGC have the same ratio of diameter to height (3:4 for base and 2:3 for subgrade). Figure 3 shows the impact hammer mold with 6 in. diameter and the SGC mold with 5.9 in diameter used in this study.

Figure 3. Molds for Impact Hammer and SGC Compactions.

Compaction Parameters

Since there are no standard test procedures to compact base and subgrade materials with the SGC, researchers developed the SGC compaction procedure with applying the compaction parameters currently used for hot mix asphalt (HMA) compaction, including Tex-241-F, AASHTO T312, and ASTM D6925 (*8*, *9*, *10*). The compaction pressure was set to 600 kPa (87 psi), but if a specimen failed to reach the specified height after applying a maximum gyration number in the SGC, a new sample was compacted with increased compaction pressure in increment of 100 kPa. For the gyration angle, the test procedures defines to mold the specimens at internal angle of $1.16 \pm 0.02°$. However, the external angle mode should be used for the

subgrade soil since the internal angle mode is not supported with the 100 mm mold size in the Pine AFG2 gyratory compactor. Also, ASTM D 6925 recommends to use an angle of 1.25 ± 0.02° if the external angle is chosen for SGC operation (*10*).

The compaction mode should be height controlled to compact samples with pre-determined maximum density, which allows compaction to proceed until reaching a specified height. Table 3 lists the compaction parameters used to compact the base and subgrade materials with the SGC. Figure 4 shows the compaction parameters set in the Pine AFG2 gyratory compactor.

Table 3. Parameters for Use in Applying SGC to Soil and Base Compaction.

Variables		Levels/Values	Note
Compaction Pressure		600 kPa (87 psi)	
Gyration angle	Base	1.16 ± 0.02°	Internal angle
	Subgrade	1.25 ± 0.02°	External angle
Gyration rate		30 gyration per minute	
Compaction mode		Height controlled	
Specimen Size	Base	150 mm (5.91 in.) dia.×200 mm (7.87 in.) tall	
	Subgrade	100 mm (3.94 in.) dia.×150 mm (5.91 in.) tall	
Water content		OMC	By Tex-113-E for base & Tex-114-E for subgrade
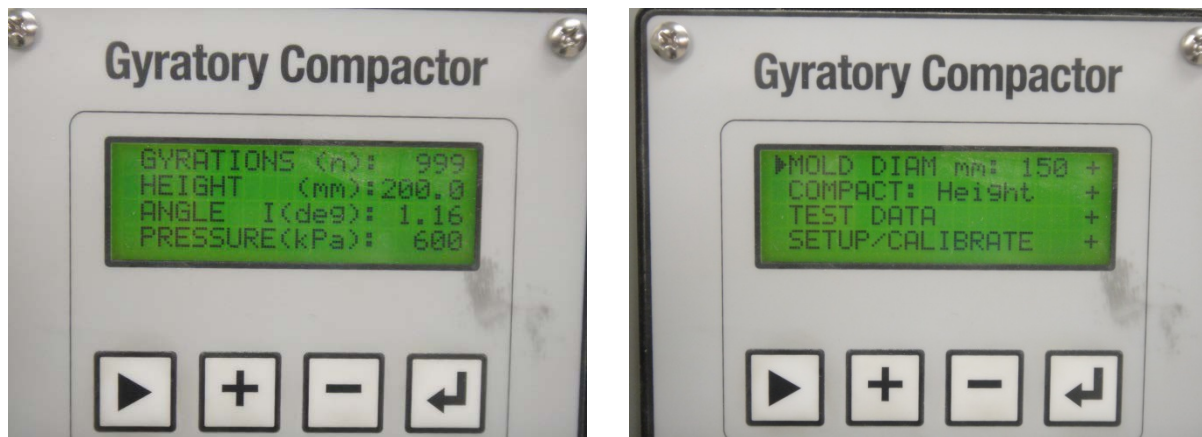
Figure 4. Compaction Parameters in Pine AFG2 Gyratory Compactor.

Compaction Procedures

Using the SGC compaction parameters presented in Table 3, researchers prepared test specimens for compressive strength test at the OMC predetermined from Tex-113-E or Tex-114-E. The general SGC compaction procedure for base and subgrade materials follows:

1. Using the OMC and MDD determined by Tex-113-E (for flexible bases) and Tex-114-E (for soils), calculate the corrected mass of water and air-dried material required for SGC mold size.

a. Base material: 150 mm (5.91 in.) diameter × 200 mm (7.87 in.) height.
b. Subgrade soil material: 100 mm (3.94 in.) diameter × 150 mm (5.91 in.) height.
2. Weigh and mix the water and material, and stand for 18–24 hr.
3. Prepare sample in SGC mold.
   a. For base material, after dividing material passing and retained on 7/8 in. sieve into four equal portions, and construct all four layers in the SGC mold, as described in Tex-113-E Section 6.16 (Figure 5).

Figure 5. Sample Preparation of Base Material.

b. For subgrade materials, pour all material in the SGC mold.
c. When material is extended above the mold, press the material into mold by hand or a slide hammer.
4. Set the compaction parameter of SGC, as listed in Table 3.
5. Insert the mold into the chamber and start the gyratory compaction (Figure 6). If the specimen fails to reach the specified height after applying the maximum number of gyrations, set higher compaction pressure in increments of 100 kPa and compact a new sample.

Figure 6. Extruding Sample from SGC and Placing a Triaxial Cell.

6. Immediately after recording the weight, enclose the specimen in a triaxial cell with porous stones and paper discs on top and bottom.
7. Allow the specimen to set 24 hours at room temperature, and then perform the compressive strength test in accordance with the test method Tex-117-E Part 2.

The steps for constructing samples in the SGC mold is similar to the test method Tex-113-E or Tex-114-E, but the SGC sample in the mold should be constructed in four layers but compacted in one lift, as illustrated in Figure 7.

Impact Hammer Compaction (Tex-113/114-E)

Compact 4

Compact 3

Layer 4

Compact 2

Layer 3

Compact 1

Layer 2

Layer 1

SGC Compaction

Compact 1

Layer 4

Layer 3

Layer 2

Layer 1
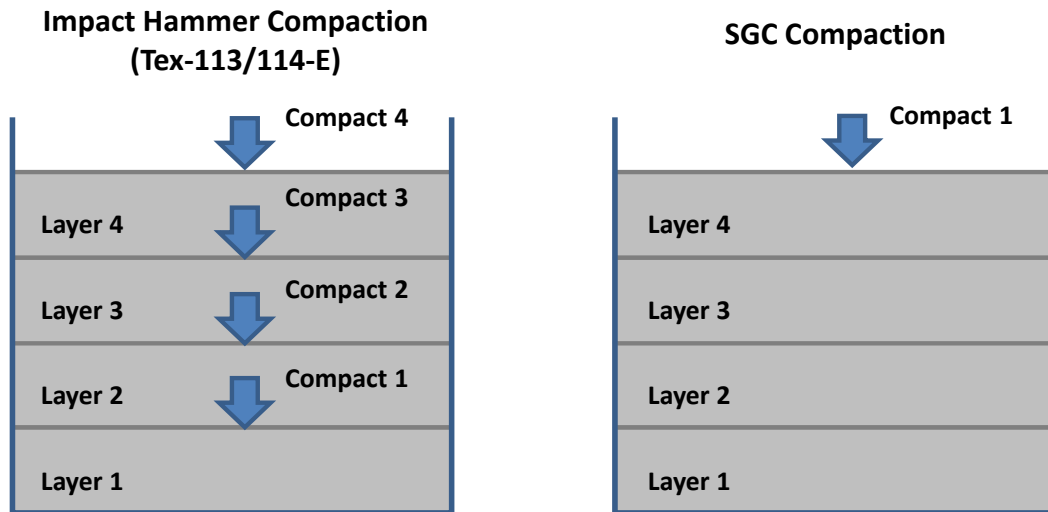
Figure 7. Sample Preparation and Compaction Scheme: Impact Hammer versus SGC.

UNCONFINED COMPRESSIVE STRENGTH TEST

To investigate whether the SGC compaction enables improved precision of compressive strength tests, unconfined compressive strength (UCS) tests were conducted in accordance with test procedure Tex-117-E Part 2 using the specimens compacted with the impact hammer and SGC. With the compressive strengths, molded moisture content and dry density of each sample were also determined and evaluated to explore the effect of compaction methods. The test results were statistically evaluated to determine if the SGC compaction yields improved, equivalent, or reduced precision and variability as compared to the impact hammer compaction.

Compressive Strength Results and Analysis

Table 4 presents all of UCS test results, and Figure 8 shows the average results including standard error bars and the standard deviation and coefficient variance (CV), respectively. The standard deviation is a common indicator of precision, quantifying the amount of variation of UCS values. On the other hand, the CV normalizes the standard deviation to the mean, being useful particularly if standard deviation increases with increasing average test value, and describes the extent of variability in relation to the mean of UCS values in this analysis. Thus, the precision of the test results can be evaluated with the standard deviation and the CV; that is, lower CV and standard deviation indicate lower scatter and higher precision in the test results.

From Figure 8(a), the materials compacted with the SGC show lower compressive strength than materials compacted with the impact hammer, except for the Amarillo material. However, as illustrated in Figure 8(b) and (c), the standard deviation and CV of UCS for the SGC compaction are lower than those for the impact hammer compaction. The results indicated that the SGC compaction enables less variability and improved precision compared to the impact hammer compaction.

Table 4. Unconfined Compressive Strength Test Results.

Sample	Base Material										Subgrade	
	Pharr		Waco		Atlanta		Amarillo		San Antonio			
	Impact	SGC	Impact	SGC	Impact	SGC	Impact	SGC	Impact	SGC	Impact	SGC
1	73.17	40.05	39.69	30.73	26.54	18.99	3.26	2.53	31.94	32.56	39.87	35.17
UCS (psi) 2	73.70	41.51	38.42	23.17	16.59	19.65	4.12	4.43	34.92	32.30	37.21	32.64
3	71.70	41.19	26.18	24.53	19.94	23.49	2.29	4.48	29.11	34.27	37.47	33.82
4	79.91	43.93	32.32	31.01	-	-	2.53	4.03	46.96	37.14	33.96	33.75
Average	74.62	41.67	34.16	27.36	21.02	20.71	3.05	3.87	35.73	34.07	37.13	33.84
Standard Deviation	3.62	1.63	6.21	4.10	5.06	2.43	0.82	0.91	7.85	2.22	2.43	1.04
Coefficient of Variance (%)	4.86	3.92	18.19	14.97	24.07	11.73	26.99	23.58	21.98	6.53	6.54	3.06
Standard Error	1.812	0.817	3.107	2.048	2.921	1.403	0.412	0.456	3.927	1.112	1.214	0.518
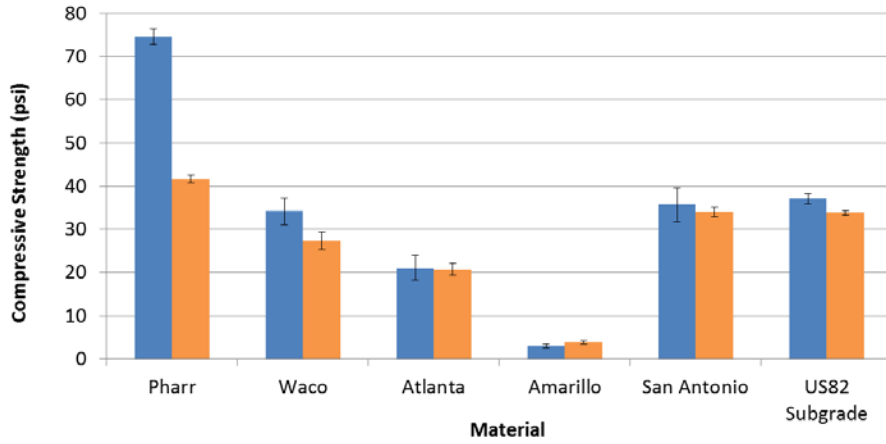
(a) Unconfined Compressive Strength
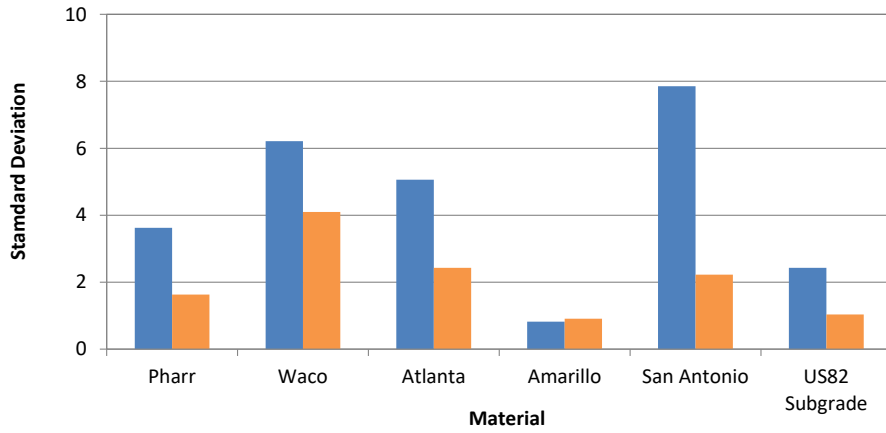
(b) Standard Deviation
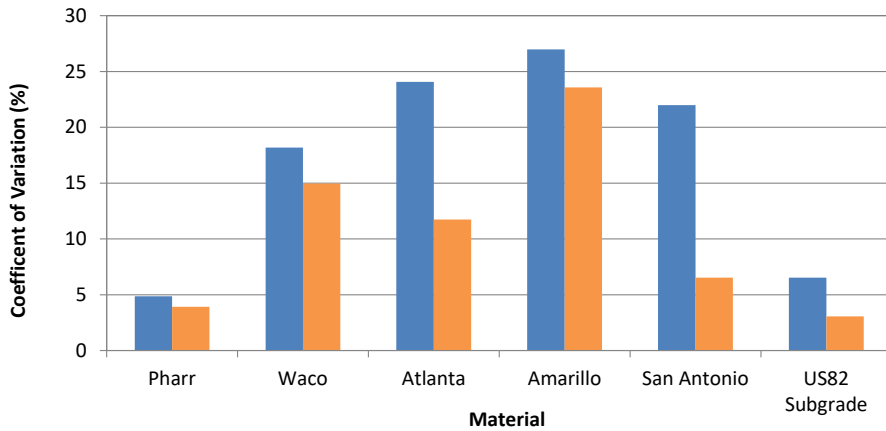
(c) Coefficient of Variation

Figure 8. Test Results of Unconfined Compressive Strength Tests.

From the comparison of standard deviation and CV, researchers proved that the SGC compaction yields less variability and improved precision for compressive strength test than the impact hammer compaction. Additionally, the *t*-test with 95 percent confidence level (CL) has been conducted to evaluate the averaged UCS test results in the two independent (compaction method) groups. In the *t*-test, the hypotheses were defined as:

- Null hypothesis (H_0) : $UCS_{hammer} = UCS_{SGC}$.
- Alternative hypothesis (H_1) : $UCS_{hammer} \neq UCS_{SGC}$.

The validity of the null hypothesis (H_0) is evaluated against alternative hypothesis (H_1) for the studied materials, as shown in Table 5. Using the experimental data, the null hypothesis (H_0) was rejected in favor of alternative hypothesis (H_1) for the Pharr base and for the subgrade material. On the other hand, it was not rejected for San Antonio, Waco, Atlanta, and Amarillo base materials. These results indicate that the averaged UCS test results from the SGC compaction are not statistically different with the test results from the impact hammer compaction except for the Pharr and subgrade materials.

Table 5. *t*-Test Outputs for Unconfined Compressive Strength Test Results.

Material	Base Materials										Subgrade	
	Pharr		Waco		Atlanta		Amarillo		San Antonio			
	Impact	SGC	Impact	SGC	Impact	SGC	Impact	SGC	Impact	SGC	Impact	SGC
Avg. UCS (psi)	74.6	41.7	34.2	27.4	21.0	20.7	3.1	3.9	35.7	34.1	37.1	33.8
Variance	13.1	2.7	38.6	16.8	25.6	5.9	0.6	0.8	61.7	5.0	5.9	1.1
Pooled Variance	7.899		27.690		15.752		0.754		33.304		3.483	
t-statistic	16.581		1.826		0.096		-1.331		0.408		2.489	
$t_{\alpha/2,\,n1+n2-2}$	2.447		2.447		2.776		2.447		2.447		2.447	
Reject H_0	Yes		No		No		No		No		Yes	

Also, an *F*-test on the pooled variance was conducted to compare the dispersion of the UCS test results between the specimens compacted with the impact hammer and SGC. In the *F*-test, the null hypothesis (H_0) states that the variance of UCS is statically the same for the samples made with the two compaction methods while alternative hypothesis (H_1) states that the variance for the SGC compaction is lower than impact hammer compaction as:

- Null hypothesis (H_0) : $\sigma^2_{Hammer} = \sigma^2_{SGC}$.
- Alternative hypothesis (H_1) : $\sigma^2_{Hammer} \neq \sigma^2_{SGC}$.

CLs for the *F*- test used were 95 percent. As presented in Table 6, the *F*-test results showed that null hypothesis (H_0) is rejected in favor of the alternative hypothesis (H_1), which means that the pooled variance of UCS results on the samples compacted with the SGC is statically lower than impact hammer compaction with 95 percent of CL. These results indicated that the SGC compaction resulted in lower dispersion in the UCS test results compared to the impact hammer compaction.

16

Table 6. Statistical Analysis for Equality of Variance of Strength Test Results.

Material	Base Materials										Subgrade	
	Pharr		Waco		Atlanta		Amarillo		San Antonio			
	Impact	SGC	Impact	SGC	Impact	SGC	Impact	SGC	Impact	SGC	Impact	SGC
Avg. UCS (psi)	74.6	41.7	34.2	27.4	21.0	20.7	3.1	3.9	35.7	34.1	37.1	33.8
Variance	13.1	2.7	38.6	16.8	25.6	5.9	0.6	0.8	61.7	5.0	5.9	1.1
Pooled variance of hammer ($\sigma_{p\,hammer}^2$)	24.16											
Pooled variance of SGC ($\sigma_{p\,SGC}^2$)	5.32											
F-statistic	2.27											
Reject H_0	Yes											

Comparison of Moisture Content and Dry Density

With the compressive strengths, molded moisture content and dry density of each sample were measured at the time of UCS testing to explore the effect of compaction methods. Table 7 presents moisture content and dry density of each molded sample, and Figure 9 shows the comparison of averaged moisture content and dry density by the compaction methods. The comparison indicates that both compaction methods showed similar moisture content and dry density of samples prepared with the impact hammer and SGC. Thus, the differences in the compressive strengths by the compaction method are not functions of variations in water content or density of samples.

Table 7. Measurement of Molded Moisture Content and Dry Density.

| Material		Base Materials										Subgrade	
		Pharr		Waco		Atlanta		Amarillo		San Antonio			
		Impact	SGC	Impact	SGC	Impact	SGC	Impact	SGC	Impact	SGC	Impact	SGC
Moisture Content (%)	1	12.32	12.94	7.968	8.09	5.95	5.85	4.655	4.82	6.32	5.83	20.62	19.52
	2	12.14	12.85	8.021	7.99	5.94	5.99	4.825	4.85	6.29	5.95	20.68	20.83
	3	11.98	12.88	8.048	8.15	5.83	6.00	4.778	4.86	6.41	6.11	20.61	20.56
	4	12.51	12.88	8.011	8.02	-	-	4.801	4.87	6.18	5.93	20.89	20.22
Average		12.24	12.89	8.01	8.06	5.91	5.95	4.76	4.85	6.30	5.95	20.70	20.28
Stand. Dev.		0.23	0.04	0.03	0.07	0.07	0.08	0.08	0.02	0.09	0.12	0.13	0.567
Dry Density (pcf)	1	113.8	112.2	134.8	130.3	135.5	132.7	139.9	137.8	135.8	138.3	97.9	101.6
	2	114.4	112.4	134.6	129.7	135.0	133.4	140.1	138.2	138.7	136.4	97.0	100.1
	3	113.5	112.3	133.8	130.7	136.5	133.2	140.9	138.3	137.4	136.6	97.5	100.2
	4	113.4	112.3	135.3	129.9	-	-	138.2	138.2	136.6	138.1	97.0	99.8
Average		113.8	112.3	134.6	130.1	135.7	133.1	139.8	138.1	137.1	137.3	97.4	100.5
Stand. Dev.		0.4	0.1	0.7	0.4	0.8	0.3	1.1	0.2	1.3	1.0	0.4	0.8
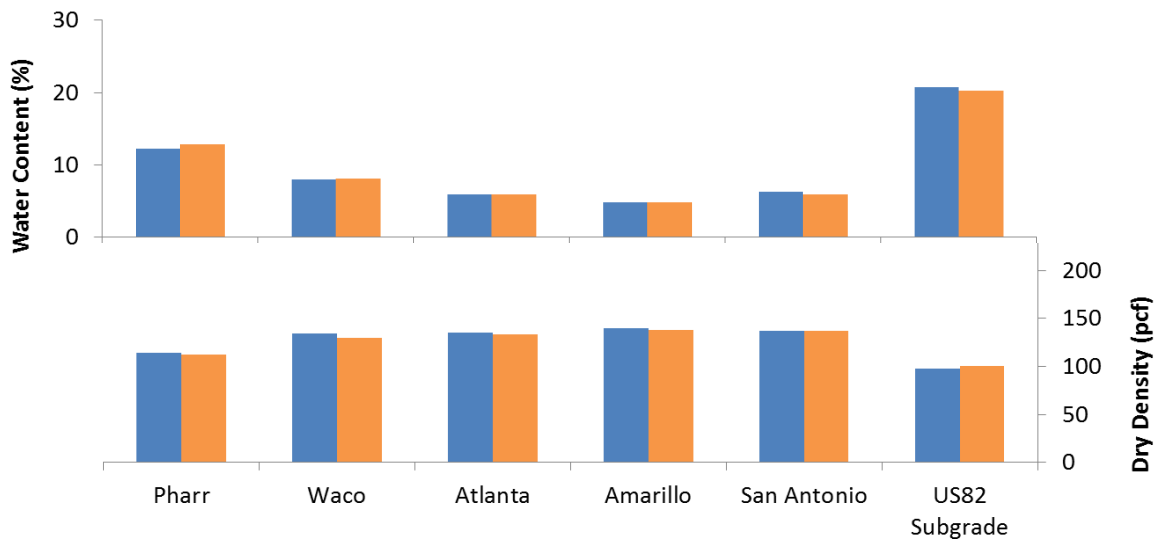
Figure 9. Comparison of Water Content and Dry Density by Compaction Methods.

SUMMARY

This chapter described whether the SGC compaction enables improved precision of the compressive strength test as compared to compaction with the impact hammer for base and

subgrade materials. The works for the measurements of compressive strength are summarized as follows:

- For the compressive strength testing, researchers collected five flexible base materials from Pharr, Waco, Atlanta, Amarillo, and San Antonio and one subgrade soil from Paris with assistance of TxDOT.
- The specimen size for SGC compaction was 150 mm (5.91 in.) diameter × 200 mm (7.87 in.) tall for base and 100 mm (3.94 in.) diameter × 150 mm (5.91 in.) tall for subgrade soil.
- The compaction parameters to compact samples with SGC as:
  - Compaction pressure: 600 kPa.
  - Gyration angle: 1.16° internal for base and 1.25° external for subgrade.
  - Gyration rate: 30 gyrations per minute.
  - Compaction mode: height controlled (200 mm for base and 150 mm for subgrade).
  - Gyration number: up to maximum of SGC machine.
- The SGC compaction procedure is similar with the Tex-113-E or Tex-114-E. However, the sample in the SGC mold should be constructed in four layers but compacted in one lift.
- While the materials compacted with the SGC showed slightly lower compressive strength than materials compacted with the impact hammer, the *t*-test indicated that for a majority of the materials the average strength test results from the SGC compaction are not statistically different with the test results from the impact hammer compaction.
- The comparisons of standard deviation and the CV show that the SGC compaction enables less variability and improved repeatability compared to the impact hammer compaction. Also, the F-test results showed that the SGC compaction led to lower dispersion in the results compared to impact compaction.
- The molded moisture contents and dry density of the test samples show similar measurements between SGC and impact hammer compactions.

CHAPTER 3. DEVELOPMENT FOR PROCEDURE FOR MOISTURE-DENSITY CURVES WITH SGC

OVERVIEW

This chapter presents findings evaluating the development of moisture-density curves with SGC. For reference, curves developed with Tex-113-E were also developed. To accomplish this objective, researchers performed the following activities:

- Recommended compaction parameters, based on prior work described in Chapter 2, to attain the applicable maximum density using the SGC.
- Performed the compaction of the base and soil materials at different water contents using the SGC to develop moisture-density curves for each material.
- Applied standard statistical paired *t*-tests to determine if the MDD and OMC were equivalent between the SGC and the applicable test method using the impact hammer.

RECOMMENDATION OF SGC PARAMETERS FOR MOISTURE-DENSITY CURVES

To begin work with the SGC to develop moisture-density curves for base and soils materials, researchers obtained the compaction parameters recommended as described in Chapter 2. The compaction parameters included compaction pressure, the number of gyrations, gyration angle, and gyration rate.

Compaction Pressure

Researchers developed the SGC compaction procedure with the compaction pressure of 600 kPa (87 psi), the gyration angle of 1.16° (internal), and the gyration rate of 30 gyrations per minute. Those compaction procedure and parameters adhere to the Superpave standards including Tex-241-F, AASHTO T312, and ASTM D6925 (*8, 9, 10*). However, the compaction pressure of 600 kPa was not sufficient to compact two base materials collected from Pharr and San Antonio to the target specimen height (150 mm). So researchers applied 800 kPa of compaction pressure for those two base materials.

Gyration Number

While the compressive strength test samples were molded with the height mode that is normally used when molding samples for performance testing, the gyration mode should be used to develop moisture-density curves with the SGC. The gyration mode allows compaction to proceed until completion of the specified number of gyration and is normally used to mold samples for volumetric properties (*8*). The gyration number required was determined using SGC densification data obtained during the compressive strength test sample compaction. Researchers observed that each material had different gyration numbers required at compactions to reach the target height (150 mm for base and 100 mm for subgrade soil). To obtain the gyration number of each material for the SGC moisture-density curve testing, researchers averaged the gyration numbers that had been applied to compact strength test samples. Figure 10 shows the densification data and averaged gyration number recommended for all materials.

(a) Pharr Base

(b) Waco Base

(c) Atlanta Base

(d) Amarillo Base

(e) San Antonio Base

(f) Paris Subgrade Soil
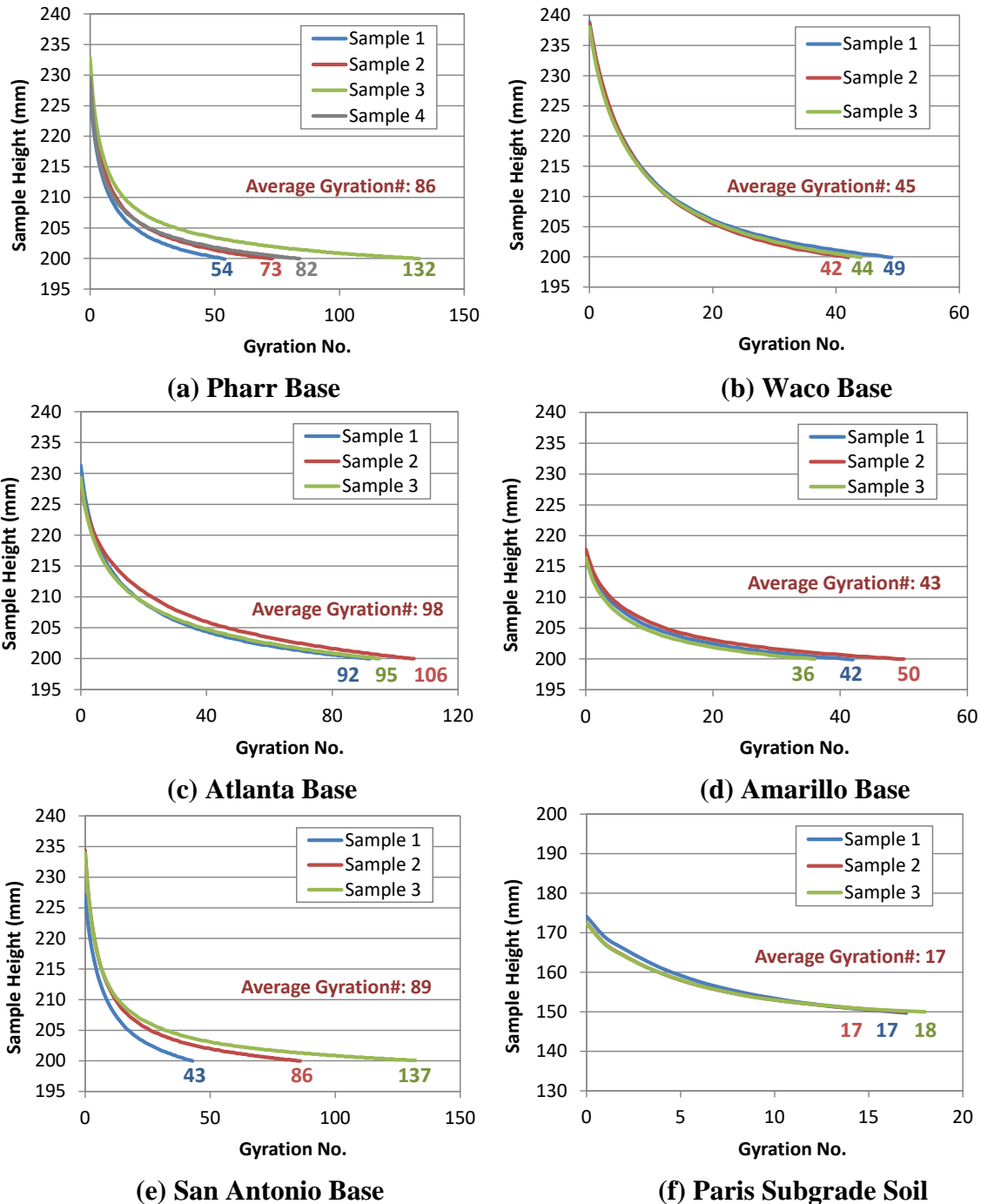
Figure 10. Gyration Number for SGC Moisture-Density Curve Testing.

Gyration Angle

While the internal 1.16° of gyration angle was applied to compact all base materials, the external angle mode was used for the subgrade soil since the internal angle mode is not supported with the 100 mm mold size in the gyratory compactor. Table 8 lists all compaction parameters recommended from the previous chapter to attain the applicable OMC and MDD using the SGC.

Table 8. SGC Compaction Parameter.

Material		Pressure (kPa)	Gyration number	Gyration angle	Gyration rate
Base	Pharr	800	86	Internal 1.16°	30 gry./min
	Waco	600	45		
	Atlanta	600	98		
	Amarillo	600	43		
	San Antonio	800	89		
Subgrade	Paris	600	17	External 1.25°	30 gry./min

DEVELOPMENT OF MOISTURE-DENSITY CURVES WITH SGC

Materials and Sample Sizes

Researchers used five flexible base materials and one subgrade soil. First, the OMC and MDD were determined based on Tex-113-E for base and Tex-114-E for subgrade soil materials, as shown in Table 9.

Table 9. Properties of Materials Used to Develop Moisture-Density Curve with SGC.

Material		Material Type		M-D Curve by Tex-113/114-E	
		Type	Grade	Dry Density (pcf)	Water Content (%)
Base	Pharr	Caliche	-	112.62	12.78
	Waco	Sandstone	Grade 4	130.95	8.21
	Atlanta	Sandstone	Grade 5	134.30	6.67
	Amarillo	Gravel	Grade 4	138.63	5.19
	San Antonio	-	Grade 2	137.47	6.48
Subgrade	Paris	Plastic Index=33		110.29	20.39

Based on the Tex-113 and 114-E, the material for moisture-density curve testing should be compacted in a 6 in. diameter × 8 in. tall mold for base material and a 4 in. × 6 in. for subgrade soil. However, since the AFG2 Gyratory Compactor used for the study supports the mold sizes of 150 mm (5.91 in.). × 200 mm (7.87 in.) for base and 100 mm (3.94 in.) × 150 mm (5.91 in.) for subgrade soil, researchers compacted the samples using those smaller molds for SGC compaction.

Procedure for Moisture-Density Curves with the SGC

Using the SGC compaction parameters in Table 8, researchers performed the compaction of base and soil materials at four different water contents using the SGC to develop moisture-density curves for each material. The general compaction procedure employed with the SGC moisture-density curve testing follows:

1. Based on the OMC and MDD determined by Tex-113-E (for flexible bases) and Tex-114-E (for soils), re-calculate the corrected mass of water and material required for SGC mold size.
   a. Base material: 5.91 in. (150 mm) D. × 7.87 in. (200 mm) Ht.
   b. Subgrade soil material: 3.94 in. (100 mm) D. × 5.91 in. (150 mm) Ht.
2. Weigh and mix the water and material, and stand for 18–24 hr.
3. Prepare sample in SGC mold.
   a. For base material, after dividing material passing and retained on 7/8 in. sieve into four equal portions, and construct all four layers in the SGC mold, as described in Tex-113-E Section 6.16.
   b. For subgrade materials, pour all material in the SGC mold.
   c. When material is extended above the mold, press the material into mold by hand or a slide hammer.
4. Set the compaction parameter of SGC, as listed in Table 8.
5. Insert the mold into the chamber and start the gyratory compaction, compacting all the material in one lift.
6. Extrude the specimen from the mold after completing the compaction.
7. Weigh the wet specimen immediately after extruding.
8. Weigh the oven-dried material, as described Tex-113-E Section 6.34–6.39 for base material and Tex-114-E Section 7.30–7.34.

Operators observed that the gyratory compaction procedure was considerably simpler compared to Tex-113/114-E due to the ease of sample preparation in the mold. Most of all, since the procedure does not require to compact lift by lift, gyratory compaction is faster than the impact hammer compaction. Figure 11 illustrates the steps taking place in a compaction sequence using the Pine AFG2 gyratory compactor.

**Figure 11. Key Steps in Compacting Base/Soil Materials with SGC.**

Moisture-Density Curves with SGC

After completing sample compaction and weight measurements at four different water contents, researchers constructed the moisture-density curves, plotting the dry density versus the percent

of molding moisture on Form Tx113_4 for each compacted specimen. Figure 12 illustrates the moisture-density curves, and Table 10 presents the OMC and MDD determined by the SGC compaction and the Tex-113/114-E (by impact hammer). These results show:

- For all flex base materials, the OMC and MDD of SGC compaction is slightly higher than ones of impact hammer compaction.
- For the subgrade soil, the OMC of SGC compaction is higher than one of impact hammer while the MDD of SGC compaction is lower.

Typically, at increasing compaction effort, the OMC is decreased while the MDD is increased (*11*). That is, the moisture-density curve is not a unique soil characteristic but depends on the compaction effort. Based on this principle of compaction effort, for the subgrade soil, the compaction effort of impact hammer is higher than one of SGC since the impact hammer compaction produced higher MDD and lower OMC. However, the principle cannot be applied to compare moisture-density curves of base materials since the SGC compaction produced higher values for both OMC and MDD. The compaction mechanism of gyratory compactor is totally different than the impact hammer. The equivalency between the SGC and impact hammer was evaluated for the flex base materials using the paired *t*-test.
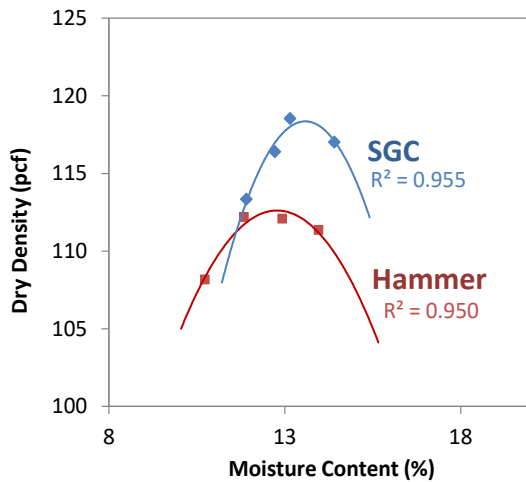
(a) Pharr Base
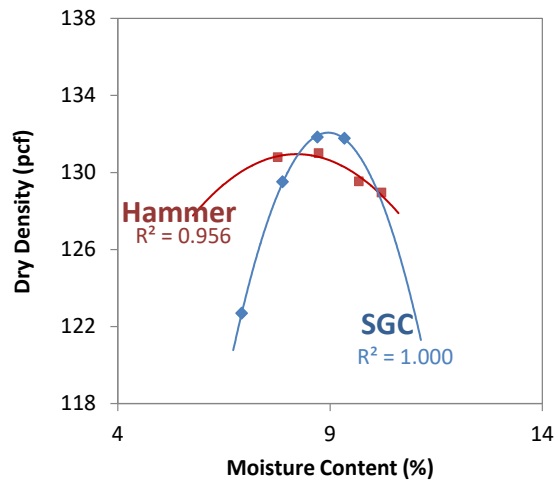
(b) Waco Base
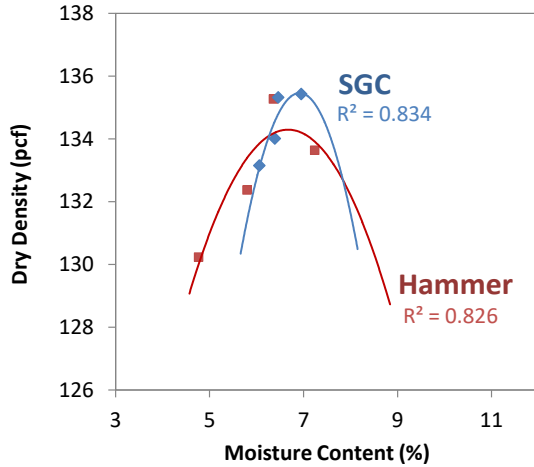
(c) Atlanta Base
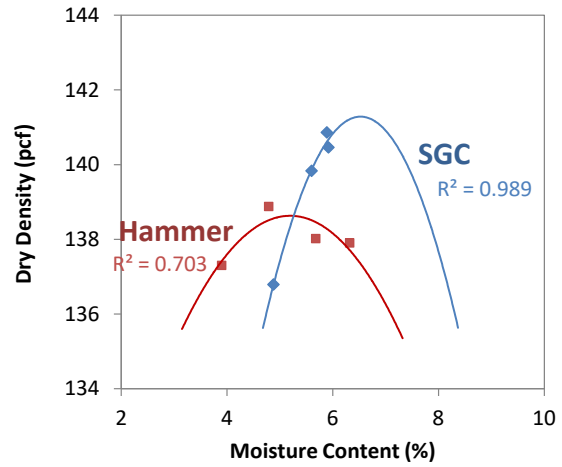
(d) Amarillo Base
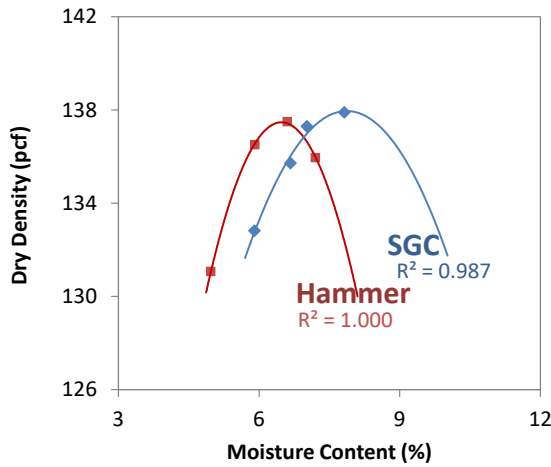
(e) San Antonio Base
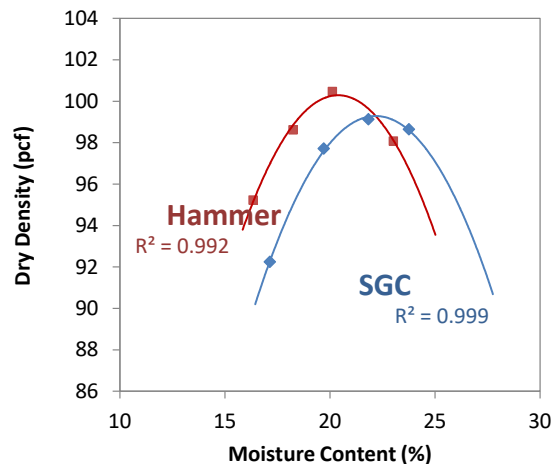
(f) Paris Subgrade Soil

Figure 12. Moisture-Density Curves of Impact Hammer and SGC.

Table 10. Moisture Content and Dry Density by Tex-113/114-E (Impact Hammer) and SGC.

Material		Opt. Moisture Content (%)		Max. Dry Density (pcf)	
		Tex-113/114-E	SGC	Tex-113/114-E	SGC
Base	Pharr	12.78	13.58	112.62	118.36
	Waco	8.21	8.96	130.95	132.07
	Atlanta	6.67	6.91	134.30	135.46
	Amarillo	5.19	6.53	138.63	141.29
	San Antonio	6.48	7.87	137.47	137.96
Subgrade	Pairs	20.39	22.18	100.29	99.29

STATISTICAL ANALYSIS OF MOISTURE-DENSITY CURVES

To investigate if the OMC and MDD of flex base materials are statistically equivalent or different between the SGC and the Tex-113 or 114-E (impact hammer), the paired *t*-test was conducted. In this test, using the observed data, a null hypothesis (H_0) is tested against an alternative hypothesis (H_1) to find out which hypothesis is supported by the existing data. In these hypotheses, the effect of controlling factors can be investigated, which is compaction method. The null hypothesis expresses no effects of the controlling factors (compaction methods) on test parameters (OMC and MDD), while alternative hypothesis states that the controlling factor can affect test parameters. The paired *t*-test has been conducted with 95 percent CL (or 5 percent level of significance, α=0.05), which represents the strength of the observed data points to support or reject assumed hypotheses. The paired *t*-test results of the OMC and MDD are shown in Table 11 and Table 12, respectively.

In the paired *t*-test for OMC (Table 11), the null hypothesis (H_0) is that the OMCs from SGC and impact hammer compaction are the same while the alternative hypothesis (H_1) is that the OMC of SGC is higher than the OMC from the impact hammer. The result of the paired *t*-test for OMC shows that the null hypothesis is rejected. The data support the alternative hypothesis, which states that the OMC obtained from SGC is higher than impact hammer.

Table 11. Paired *t*-test Results of OMC between SGC and Impact Hammer Compactions.

Materials		OMC (%)		Difference of OMC (%)
		Impact Hammer	SGC	
Base	Pharr	12.78	13.58	0.80
	Waco	8.21	8.96	0.75
	Atlanta	6.67	6.91	0.24
	Amarillo	5.19	6.53	1.34
	San Antonio	6.48	7.87	1.39
Paired *t*-test Result (CL 95%, α=0.05)	Mean	-	-	0.94
	Standard Deviation	-	-	0.47
	Standard. Error	-	-	0.21
	t-statistic	-	-	4.26
	$t_{n1+n2-2,\ \alpha}$	-	-	1.86
	H_0: (OMC$_{Hammer}$) = (OMC$_{SGC}$); H_0 is rejected.			
	H_1: (OMC$_{Hammer}$) < (OMC$_{SGC}$); Data support H_1. OMC$_{SGC}$ is higher than the OMC$_{hammer}$			

In the paired *t*-test for MDD as presented in Table 12, the null hypothesis (H_0) is that the MDD of impact hammer compaction is the same as the one of SGC compaction. On the other hand, the alternative hypothesis (H_1) is that the MDD of SGC is different from the impact hammer. In this case, the result shows that the null hypothesis, stating that the MDD from the two compaction methods are the same, is rejected. The data support the alternative hypothesis, which states that the MDD obtained from the SGC is higher than the impact hammer.

Table 12. Paired *t*-test Results of MDD between SGC and Impact Hammer Compactions.

Materials		MDD (%)		Difference of MDD (%)
		Impact Hammer	**SGC**	
Base	Pharr	112.62	118.36	5.74
	Waco	130.95	132.07	1.12
	Atlanta	134.30	135.46	1.16
	Amarillo	138.63	141.29	2.66
	San Antonio	137.47	139.96	2.49
Paired *t*-test Result (CL 95%, α=0.05)	Mean	-	-	2.63
	Standard Deviation	-	-	1.88
	Standard Error	-	-	0.84
	t-statistic	-	-	3.13
	$t_{n1+n2-2,\ \alpha}$	-	-	2.31
	H_0: $MDD_{Hammer} = MDD_{SGC}$; H_0 is rejected.			
	H_1: $MDD_{Hammer} < (MDD_{SGC})$; Data support H_1. MDD_{SGC} is higher than the MDD_{hammer}			

SUMMARY

Based on the data and analysis presented, researchers drew the following conclusions:

- The following compaction parameter were recommended from Task 2 to attain the applicable maximum density using the SGC:
  - Compaction pressure: 600 or 800 kPa.
  - Gyration angle: Internal 1.16°.
  - Gyration rate: 30 gyrations per minute.
  - Gyration number: as per base/soil materials.
- The gyratory compaction procedure is simpler and faster than the Tex-113/114-E due to the ease of sample preparation and compaction.
- For all base materials, the SGC compaction produced slightly higher OMC and MDD than the impact hammer compaction. This conclusion was supported by statistical evaluation of the data. On average, the OMC from SGC compaction was about 1 percentage point higher and the MDD on average was about 2.6 pcf heavier.
- For the subgrade soil, the OMC from samples compacted with SGC is higher than one with impact hammer while the MDD with SGC is lower.

CHAPTER 4. EVALUATION OF SGC PREPARATION FOR PERFORMANCE AND M-E DESIGN

OVERVIEW

Unbound aggregate materials in pavement structures experience both recoverable and permanent deformation under repeated loading of moving vehicles (*12*). Therefore, resilient modulus and permanent deformation are primary input properties of base layers using unbound aggregate materials in M-E design methods. Also, these properties are used in structural analysis models to analyze the pavement structural responses to the traffic loads. In this chapter, the applicability of using the SGC for base materials was evaluated in context of new and emerging M-E pavement design methods. The evaluation was accomplished through the following activities:

- Measure permanent deformation and resilient modulus properties of selected base materials compacted with impact hammer and SGC.
- Compare and analyze the data to determine whether specimens compacted with the SGC yield different M-E design properties from specimens of the same material prepared with the impact hammer.
- Perform analysis using Texas M-E Thickness Design System (TxME) to evaluate influence of specimens prepared with impact hammer and SGC on M-E design properties.

In this chapter, test protocols, specimen size, testing machine, experimental results, and permanent deformation and resilient modulus models are also discussed.

MEASUREMENT OF PERMANENT DEFORMATION AND RESILIENT MODULUS

Repeated load triaxial tests were conducted to measure the permanent deformation and resilient modulus of the selected four base materials including Pharr, Waco, Atlanta, and San Antonio materials. Two series of specimens, one with SGC and the other with impact hammer compaction, were prepared and tested.

Sample Size and Testing Machine

A cylindrical specimen with 6 in. diameter and 12 in. in height is normally used to perform the repeated load triaxial tests to measure permanent strain and/or resilient modulus of base materials. However, due to the restriction in the height of SGC mold, the SGC specimens were prepared with 150 mm (5.91 in.) diameter and 200 mm (7.87 in.) height in this study. On the other hand, the size of specimen compacted with the impact hammer was 6 in (152.4 mm) in diameter and 8 in (203.2 mm) in height, which have the same ratio (diameter:height = 2:3) to remove or minimize the size effect of test specimens. Each material was weighed according to its MDD and OMC determined by Tex-113-E to make sure the samples to be compacted with the same density.

A top-loading closed loop electro-hydraulic testing machine was used in the laboratory test. The vertical deformation of the specimen was measured by two clamp-mounted linear variable differential transformers mounted on the sides of the specimens. A triaxial pressure chamber was

used in the testing machine, which contains the specimen and applied the confining pressure to the specimen using air pressure. Figure 13 illustrates the testing machine and specimen setup in the triaxial chamber.
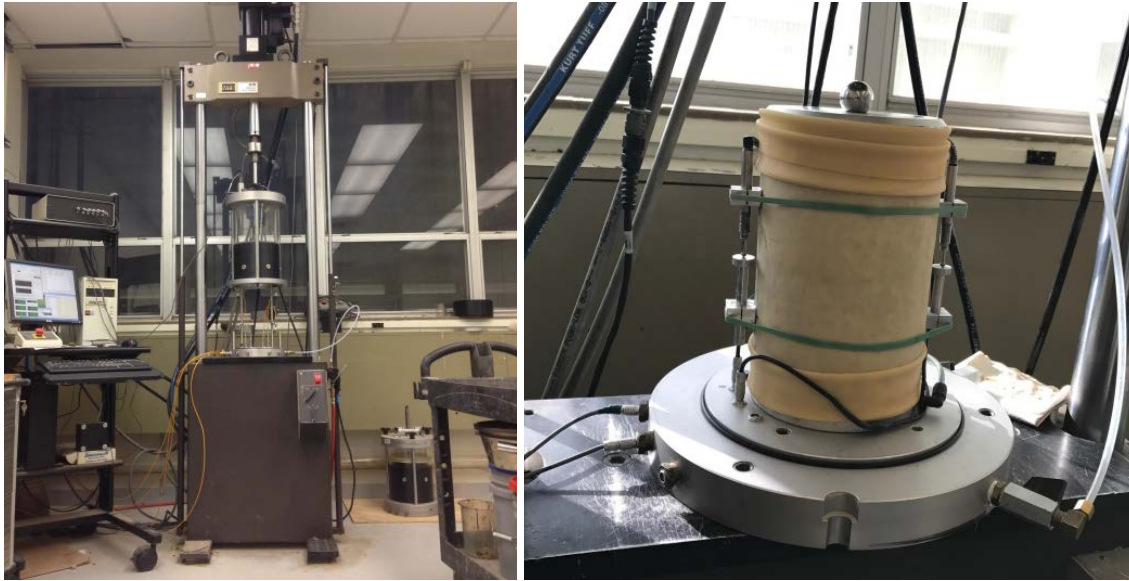

Figure 13. Hydraulic Testing Machine and Specimen Setup.

Permanent Deformation Test

While there are a few test standards for measuring the resilient modulus of unbound granular materials such as AASHTO TP31 or National Cooperative Highway Research Program (NCHRP) 1-28A, no standard test procedures were developed for evaluating permanent deformation in a laboratory condition. Instead, repeated load triaxial testing is widely used to measure permanent strain by applying a constant confining pressure in a triaxial cell and a cyclic axial stress used to simulate traffic loading.

Stress State

The stress states used to measure permanent strain included the application of 100 cycles of a 3 psi deviator stress with 15 psi confining pressure for preconditioning and 10,000 cycles of a 20 psi deviator stress with 10 psi confining pressure for repeated loading, as listed Table 13. The loading wave form is a haversine load pulse with 0.1 loading and 0.9 second rest period.

Table 13. Stress States for Permanent Deformation Test.

Loading	Confining Pressure		Contact Stress		Cyclic Stress		Maximum Stress		Nrep.
	kPa	psi	kPa	psi	kPa	psi	kPa	psi	
Precondition	103.4	15.0	20.7	3.0	20.7	3.0	41.4	6.0	100
Permanent Deformation	68.9	10.0	20.7	3.0	137.8	20.0	158.5	23	10,000

Permanent Deformation Models

In this study, VESYS and Tseng- Lytton three parameter models were used to analyze the permanent strains obtained from the repeated load triaxial test (*13*, *14*). The VESYS model is used in the TxME, and the Tseng-Lytton model is used in Mechanistic Empirical Pavement Design Guide to compute the permanent deformation of the unbound aggregate layers (*15*). The VESYS model assumes that the relation between permanent strain and number of load repetitions is linear in logarithmic scale, which is expressed as:

$$\varepsilon^p = \mu \varepsilon_r N^{-\alpha} \tag{4.1}$$

where ε^p is permanent strain, ε_r is resilient strain (at 200th load cycle), N is number of load repetitions, and α and μ are model coefficients that are used as the rutting properties of base and subgrade layers in the TxME software. The permanent deformation increases at a higher rate for the initial load cycles and at a lower rate as the number of load cycles increases. Thus, the relationship between permanent deformation and number of load cycles is expressed as:

$$\varepsilon_p = aN^b \tag{4.2}$$

From the Equation 4.2, the model coefficient α and μ are determined as:

$$\alpha = 1 - b \tag{4.3}$$

$$\pi = \frac{ab}{\varepsilon_r} \tag{4.4}$$

Tseng and Lytton developed a three parameter model using a sigmoidal curve fitting as follows:

$$\varepsilon^p = \varepsilon_0^p \, e^{-(\rho/N)^\beta} \tag{4.5}$$

where ε_0^p is maximum permanent strain, β is shape factor, and ρ is scale factor. The Tseng-Lytton model does not employ the resilient strain that is used in the VESYS model (*14*).

Test Results and Analysis

Figure 14 presents the permanent deformation responses on load repetition from the laboratory triaxial test. From the response curves, the materials compacted with the SGC were associated with lower accumulated permanent strains than ones compacted with the impact hammer, except for Pharr base material. These results suggest that the permanent deformation behavior is not a unique soil characteristic but depends on the compaction effort even though the impact hammer and SGC samples were compacted with the same density value.
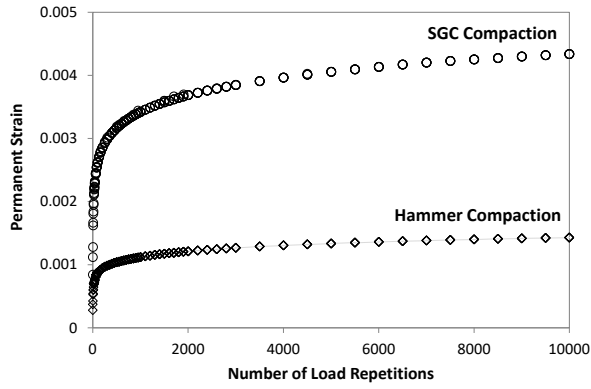
(a) Pharr
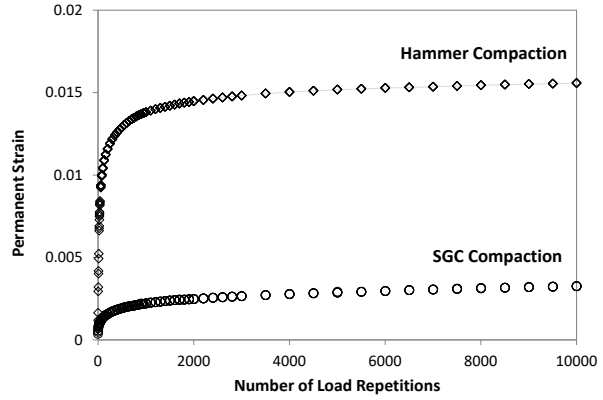
(b) Waco
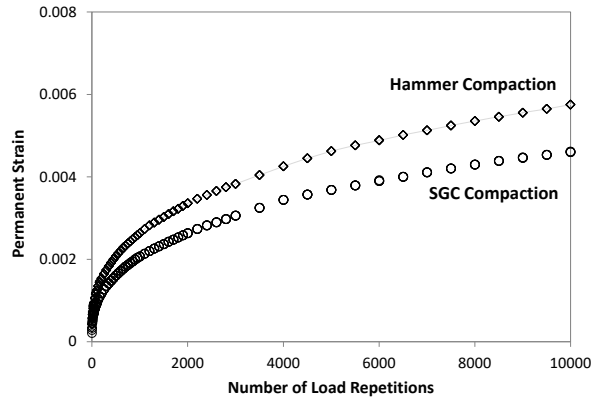
(c) Atlanta
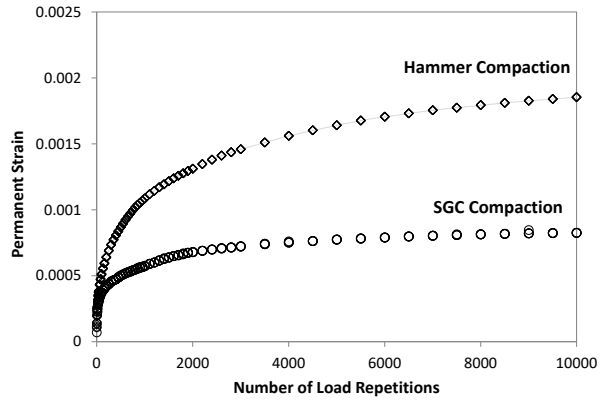
(b) San Antonio

Figure 14. Permanent Strain-Load Repetition Curves.

To determine the rutting properties required in the M-E design procedure, the test results were analyzed using the VESYS model (Equation 4.1). Figure 15 presents the permanent deformation responses measured from the laboratory and the prediction curves fitted with the Equation 4.2. Also, Table 14 presents the rutting parameters (α and μ) calculated with the VESYS model and predicted maximum permanent strains according to the material types and compaction methods. From Figure 15 and Table 14, the materials compacted with the SGC were associated with lower accumulated permanent strains than ones compacted with the impact hammer, except for Pharr base material.
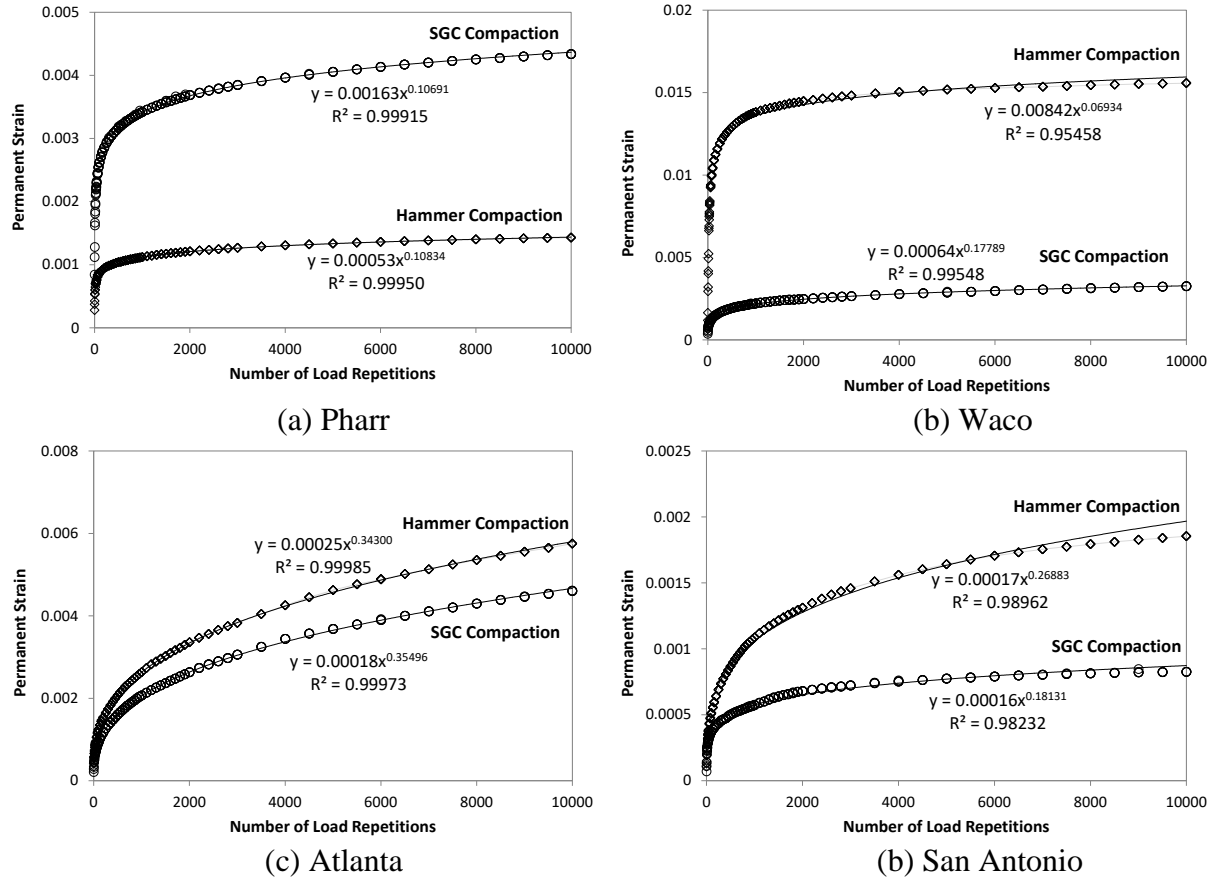
(a) Pharr	(b) Waco
(c) Atlanta	(b) San Antonio

Figure 15. Permanent Strain-Load Repetition Curves (VESYS Model).

Table 14. Rutting Parameters and Permanent Strains from VESYS Model.

Base Materials	Compaction	Max. Permanent Strain (%)	Rutting Parameters		R^2
			α	μ	
Pharr	Hammer	0.144	0.891	0.089	0.999
	SGC	0.436	0.893	0.211	0.999
Waco	Hammer	1.595	0.931	1.423	0.955
	SGC	0.329	0.822	0.417	0.995
Atlanta	Hammer	0.589	0.657	0.170	0.999
	SGC	0.473	0.645	0.150	0.999
San Antonio	Hammer	0.202	0.731	0.217	0.990
	SGC	0.085	0.819	0.191	0.982

Figure 16 illustrates the experimental test data and model outputs predicted with the Tseng-Lytton model, and Table 15 lists the results of the regression analysis based on the least mean square error method. The coefficient of determinations (R^2) between the measure and predicted data are higher than 0.95 for all specimens. Table 15 shows that the specimens compacted with the SGC have lower maximum permanent strains (ε_0^p) compared to the specimens compacted with the impact hammer, except for Pharr materials. Furthermore, lower shape factor (β) is

observed from the SGC specimens, which indicates a steeper slope at the beginning of the permanent strain curve and lower slope of the curve at the higher number of load repetitions.
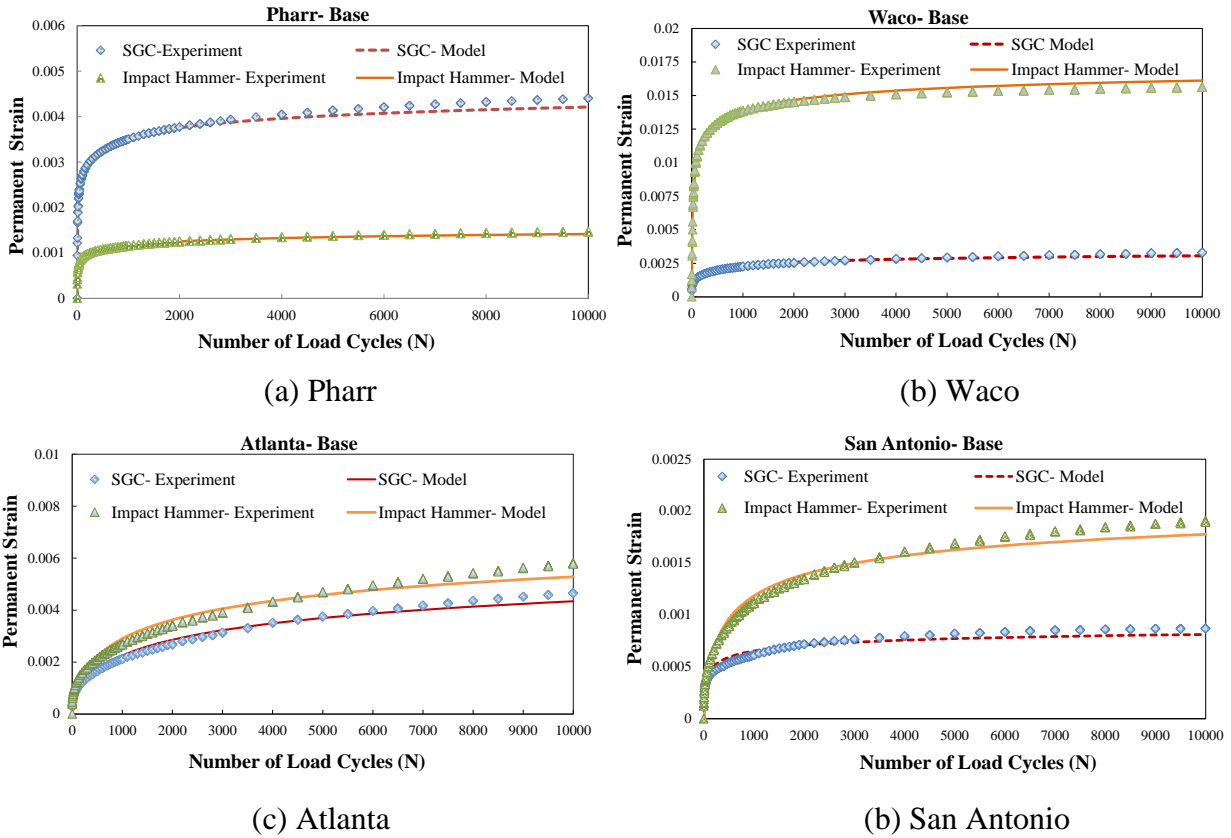

(a) Pharr

(b) Waco

(c) Atlanta

(b) San Antonio

Figure 16. Permanent Strain-Load Repetition Curves (Tseng-Lytton Model).

Table 15. Rutting Parameters and Permanent Strains from Tseng-Lytton Model.

Base Materials	Compaction	Model Parameters			R^2
		β	ρ	ε_0^p	
Pharr	Hammer	0.178	36.93	0.0020	0.995
	SGC	0.169	26.60	0.0060	0.998
Waco	Hammer	0.321	21.89	0.0185	0.996
	SGC	0.272	145.42	0.0042	0.994
Atlanta	Hammer	0.285	2177.88	0.0101	0.977
	SGC	0.265	2727.07	0.0085	0.972
San Antonio	Hammer	0.370	391.50	0.0024	0.992
	SGC	0.282	61.54	0.0010	0.973

Resilient Modulus Test

The resilient modulus is used with structural response analysis models to calculate the pavement structural response to wheel loads, and with the combination of permanent deformation properties and pavement design procedures to predict rutting performance. The repeated load triaxial test was conducted to measure the resilient modulus and investigate whether specimens

prepared with the SGC yield different modulus from specimens of the same materials prepared with the impact hammer.

Stress State

In this study, a standard test method recommended by the NCHRP Project 1-28A was used for the test procedure and loading sequence. The test procedure should be conducted by applying both cyclic and confining stress at each constant stress ratio. Both the cyclic and confining stresses are increased to maintain a constant stress ratio. Table 16 present the loading sequence used for the base materials (*16*).

Table 16. Loading Sequences used for Resilient Modulus Test.

Sequence	Confining Pressure		Contact Stress		Cyclic Stress		Maximum Stress		Nrep.
	kPa	psi	kPa	psi	kPa	psi	kPa	psi	
Precondition	103.5	15.0	20.7	3.0	20.7	3.0	41.4	6.0	100
1	20.7	3.0	4.1	0.6	10.4	1.5	14.5	2.1	100
2	41.4	6.0	8.3	1.2	20.7	3.0	29.0	4.2	100
3	69.0	10.0	13.8	2.0	34.5	5.0	48.3	7.0	100
4	103.5	15.0	20.7	3.0	51.8	7.5	72.5	10.5	100
5	138.0	20.0	27.6	4.0	69.0	10.0	96.6	14.0	100
6	20.7	3.0	4.1	0.6	20.7	3.0	24.8	3.6	100
7	41.4	6.0	8.3	1.2	41.4	6.0	49.7	7.2	100
8	69.0	10.0	13.8	2.0	69.0	10.0	82.8	12.0	100
9	103.5	15.0	20.7	3.0	103.5	15.0	124.2	18.0	100
10	138.0	20.0	27.6	4.0	138.0	20.0	165.6	24.0	100
11	20.7	3.0	4.1	0.6	41.4	6.0	45.5	6.6	100
12	41.4	6.0	8.3	1.2	82.8	12.0	91.1	13.2	100
13	69.0	10.0	13.8	2.0	138.0	20.0	151.8	22.0	100
14	103.5	15.0	20.7	3.0	207.0	30.0	227.7	33.0	100
15	138.0	20.0	27.6	4.0	276.0	40.0	303.6	44.0	100
16	20.7	3.0	4.1	0.6	62.1	9.0	66.2	9.6	100
17	41.4	6.0	8.3	1.2	124.2	18.0	132.5	19.2	100
18	69.0	10.0	13.8	2.0	207.0	30.0	220.8	32.0	100
19	103.5	15.0	20.7	3.0	310.5	45.0	331.2	48.0	100
20	138.0	20.0	27.6	4.0	414.0	60.0	441.6	64.0	100
21	20.7	3.0	4.1	0.6	103.5	15.0	107.6	15.6	100
22	41.4	6.0	8.3	1.2	207.0	30.0	215.3	31.2	100
23	69.0	10.0	13.8	2.0	345.0	50.0	358.8	52.0	100
24	103.5	15.0	20.7	3.0	517.5	75.0	538.2	78.0	100
25	138.0	20.0	27.6	4.0	690.0	100.0	717.6	104.0	100
26	20.7	3.0	4.1	0.6	144.9	21.0	149.0	21.6	100
27	41.4	6.0	8.3	1.2	289.8	42.0	298.1	43.2	100
28	69.0	10.0	13.8	2.0	483.0	70.0	496.8	72.0	100
29	103.5	15.0	20.7	3.0	724.5	105.0	745.2	108.0	100
30	138.0	20.0	27.6	4.0	966.0	140.0	993.6	144.0	100

Resilient Modulus Model

To calculate the resilient modulus and the regression parameters (k_i) used in the M-E design for predicting pavement performance, the following model proposed by NCHRP project 1-37A was used in this study (*12*):

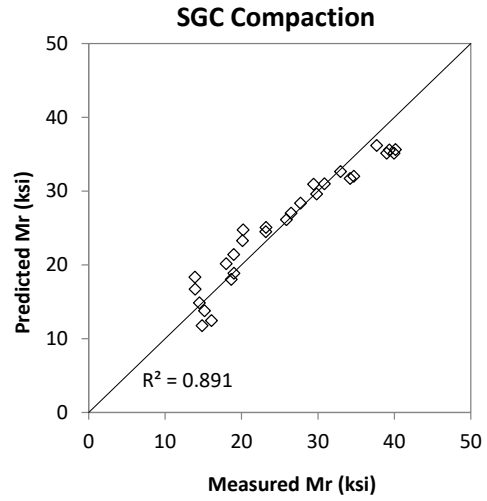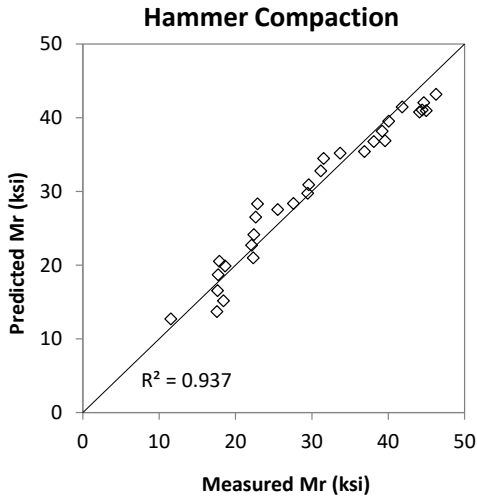$$M_r = k_1 p_a \left(\frac{\theta}{p_a}\right)^{k_2} \left(\frac{\tau_{oct}}{p_a} + 1\right)^{k_3} \tag{4.6}$$

where M_r is resilient modulus, p_a is atmospheric pressure (14.7 psi), θ is bulk stress, τ_{oct} is octahedral shear stress, and k_1, k_2, and k_3 are regression coefficients. The volumetric and deviator components of the stress tensor are normalized with atmospheric pressure. Therefore, the regression coefficients are dimensionless.
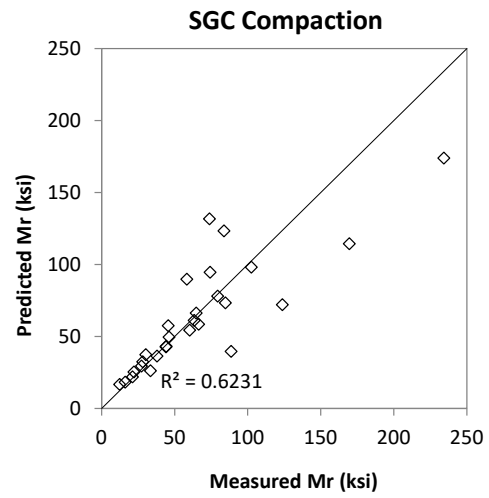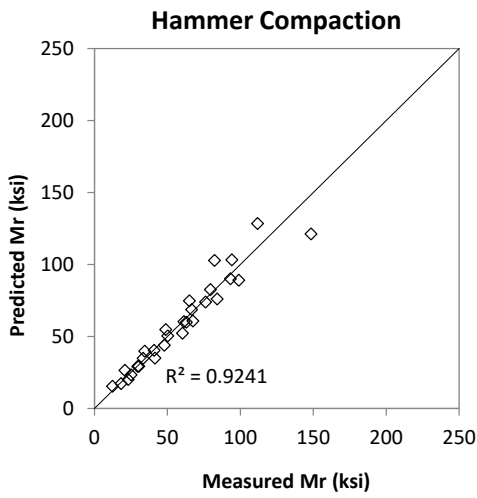
Test Results and Analysis

Table 17 lists the regression coefficients and resilient modulus at 5 psi of confining pressure and 15 psi of deviator stress calculated using the repeated load triaxial test results according to material type and compaction method. Figure 17 presents the predicted and measured resilient modulus at different stress states of each material and compaction method. The results indicate that the base material compacted with the SGC were associated with higher resilient modulus than ones compacted with the impact hammer, except for the Pharr material. Similar to results for the permanent deformation test, the resilient modulus is not a unique soil property but actually may depend on the type of lab compaction process, where the compaction process may result in changes in aggregate shape properties and thus influence the resilient modulus and the permanent deformation behavior. More details will be discussed in Chapter 5 with measured aggregate shape properties.

Table 17. Generalized Model Coefficients for Prediction of Resilient Modulus.
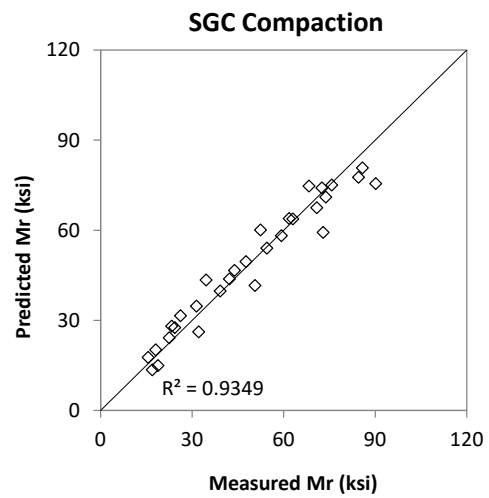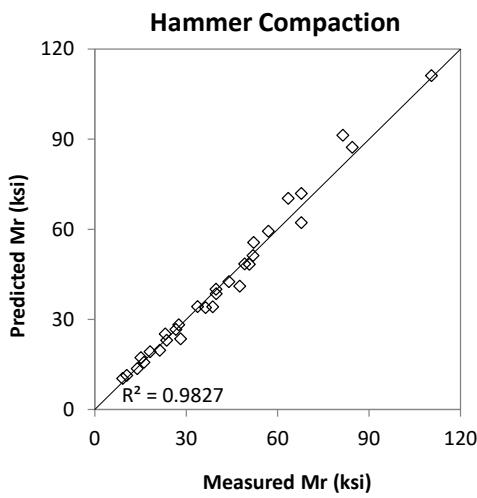
Base Materials	Compaction	Model Parameters			Modulus (ksi) at 5 psi confining pressure and 15 psi deviator stress
		k_1	k_2	k_3	
Pharr	Hammer	1094.55	0.688	-0.476	21.80
	SGC	998.00	0.660	-0.481	19.44
Waco	Hammer	1359.66	0.798	-0.029	34.90
	SGC	1369.58	0.861	-0.259	37.50
Atlanta	Hammer	874.469	0.736	0.137	22.94
	SGC	1320.90	0.998	-0.693	30.15
San Antonio	Hammer	2284.04	0.877	-0.579	49.99
	SGC	1899.54	0.579	1.227	68.33

Hammer Compaction

Predicted Mr (ksi) vs Measured Mr (ksi)
R² = 0.937

SGC Compaction

Predicted Mr (ksi) vs Measured Mr (ksi)
R² = 0.891

(a) Pharr

Hammer Compaction

Predicted Mr (ksi) vs Measured Mr (ksi)
R² = 0.9241

SGC Compaction

Predicted Mr (ksi) vs Measured Mr (ksi)
R² = 0.6231

(b) Waco

Hammer Compaction

Predicted Mr (ksi) vs Measured Mr (ksi)
R² = 0.9827

SGC Compaction

Predicted Mr (ksi) vs Measured Mr (ksi)
R² = 0.9349

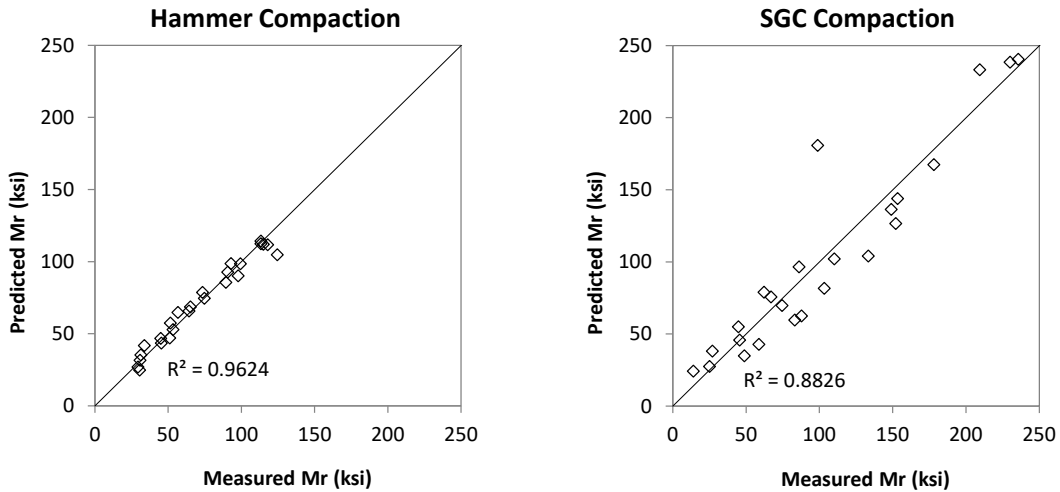**(c) Atlanta**

(d) San Antonio
Figure 17. Resilient Modulus Test Results.

SENSITIVITY ANALYSIS OF COMPACTION METHODS

As described previously, the permanent deformation behavior and resilient modulus are not unique soil characteristic in the lab but actually depends on the type of compaction process, where the compaction process can result in changes in inherent properties. The changes may influence the calculation of structural response at the design phase since both characteristics are the primary input of base layers for the M-E design method. To investigate the influence of laboratory compaction methods on the pavement response, sensitivity analysis was performed using the TxME to compare performance prediction of base layers using different rutting properties and modulus as measured by the different compaction methods. Figure 18 illustrates the TxME input screen for pavement structure and material properties.
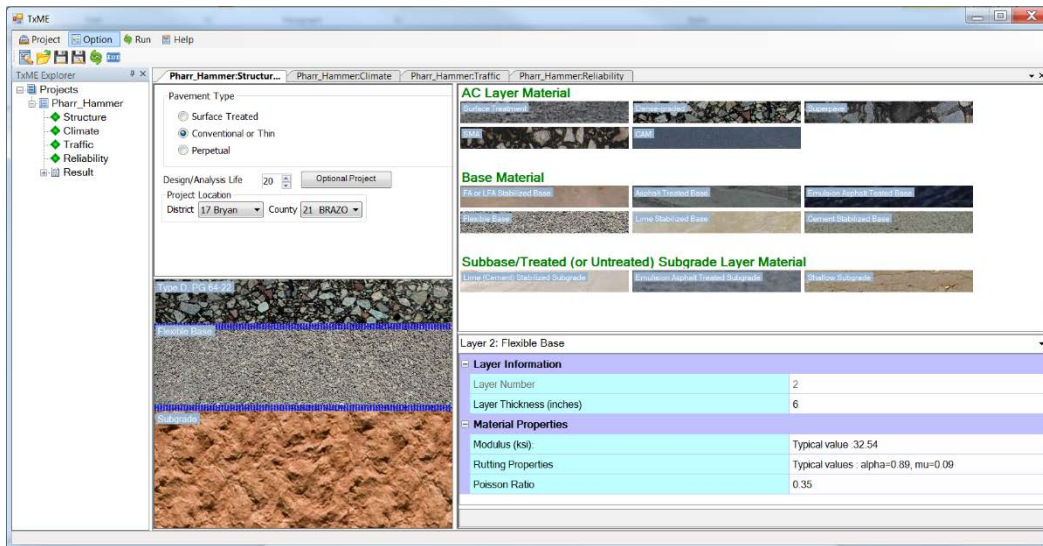

Figure 18. TxME Input Screen for Pavement Structure and Material Properties.

Input Parameters for TxME Analysis

To run the TxME software for the sensitivity analysis, input data were assumed, including pavement structure, traffic, climate, and material properties other than rutting properties and modulus of the base layer. The pavement structure consists of a 3 in. HMA surface and 6 in. flexible base, and the traffic was assumed to be 35 million of 18-kip equivalent single axle load (ESAL) at 20 years. In the analysis, much higher traffic loading was applied compared to the pavement structure (3 in. HMA surface) to cause excessive rutting in the flex base layer, which makes it easier to compare the performance prediction. The measured rutting properties and modulus values are listed in Table 18 according to material type and compaction method. Field modulus values required as the design parameter are often significantly higher than the resilient modulus measured from the laboratory testing due to differences in stress states (*17*). Thus, the NCHRP 1-37A recommends an adjustment factor of 0.40 for subgrade soils and 0.67 for granular base under flexible pavements. Table 18 provides the field modulus adjusted according to the NCHRP recommendation, which should be used as the input values in the TxME software.

Table 18. Base Material Properties Used in TxME.

Base Materials	Compaction	Rutting Properties		Modulus (ksi)	
		α	μ	Lab Value	Field Value[*]
Pharr	Hammer	0.891	0.089	21.80	32.54
	SGC	0.893	0.211	19.44	29.01
Waco	Hammer	0.931	1.423	34.90	52.09
	SGC	0.820	0.417	37.50	55.97
Atlanta	Hammer	0.657	0.170	22.94	34.24
	SGC	0.645	0.150	30.15	45.00
San Antonio	Hammer	0.731	0.217	49.99	74.61
	SGC	0.819	0.191	68.33	101.99

* Used as design modulus in TxME (Field value = Lab value/0.67)

While the rutting properties and modulus values measured in the laboratory were used for each flexible base material, default values embedded in the TxME were used for other input parameters of HMA surface and subgrade. Table 19 lists all input parameters used to predict the performance in the TxME software.

Table 19. TxME Input Data for Sensitivity Analysis.

Category	Value	Category	Value
AC Surface Information		Subgrade Information	
− Layer Thickness (in.)	3.0	− Modulus (ksi)	20
− Binder Type	PG 64-22	− Rutting Properties	0.8/0.1*
− Gradation	Type D	− Poisson Ratio	0.4*
− Dynamic Modulus	Default value		
− Fracture properties: Temp./A/n	77/4.2E-6/3.953*		
− Rutting properties: Temp./α /μ	104/0.747/0.810*	Climate (Weather Station)	College Station, TX
Flexible Bae Information		Traffic	
− Layer Thickness (in.)	6.0	− Tire Pressure (psi)	100
− Modulus (ksi)	Table 4.6	− ADT-Beginning (veh/day)	5,000
− Rutting Properties	Table 4.6	− ADT-End 20 yr (veh/day)	8,767
− Poisson Ratio	0.35*	− 18 kip ESALs 20 yr (1 dir)	35 millions
		− Operation speed (mph)	60

* Default values in TxME software

Test Results and Analysis

Figure 19 illustrates the comparison of rut depths predicted after 20 years by the TxME according to material type and compaction method. As expected, the results indicate that the base materials compacted with the SGC were associated with lower predicted rut depth since the SGC compaction resulted in lower accumulated permanent strains and higher resilient modulus, except for the Pharr material.
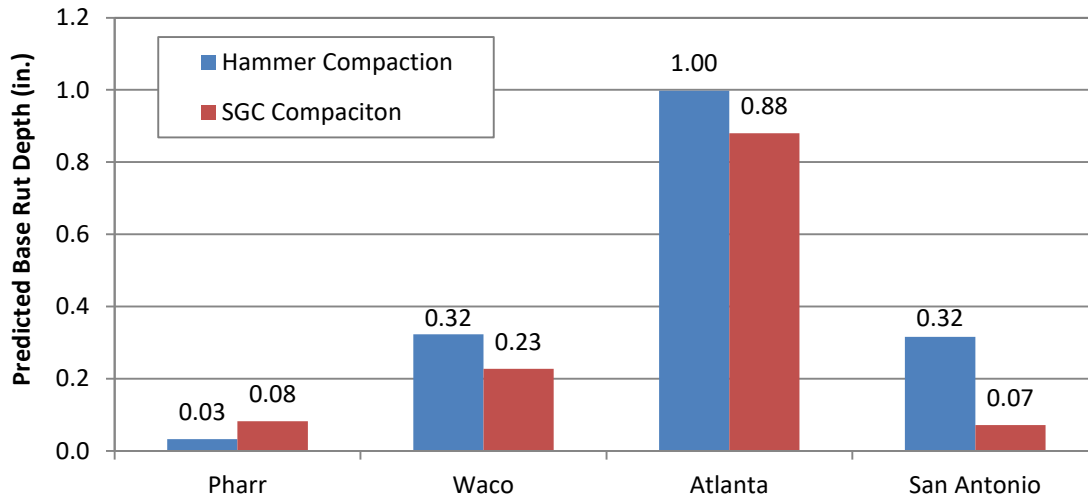

Figure 19. Rut Depth after 20 Years Predicted by TxME.

SUMMARY AND CONCLUSION

The findings from the evaluation of SGC preparation for performance and M-E design are summarized as follows:

- The repeated load triaxial testing was performed to measure permanent strains of four base materials compacted with the impact hammer and SGC.
    - From the permanent strain-load repetition curves, the materials compacted with the SGC were associated with lower accumulated permanent strains than ones compacted with the impact hammer, except for Pharr base material.
    - The permanent deformation responses measured in the lab was fitted with the VESYS and Tseng-Lytton models with higher coefficient determinations (R^2).
- The resilient moduli of the base materials were measured through the test method and loading sequence recommended by the NCHRP Project 1-28A.
    - Similar to results for the permanent deformation test, the results indicate that the base material compacted with the SGC were associated with higher resilient modulus than ones compacted with the impact hammer, except for the Pharr material.
- The results suggest that the permanent deformation and resilient modulus are not unique soil characteristics but actually may depend on the type of lab compaction process, resulting in changes in aggregate shape properties and thus influence the resilient modulus and the permanent deformation behavior.
- The sensitivity analysis using the TxME software indicated that base materials compacted with the SGC showed lower predicted rut depth since the SGC compaction resulted in lower accumulated permanent strains and higher resilient modulus, except for the Pharr material.

CHAPTER 5. EVALUATION OF MATERIAL INTERNAL STRUCTURE

OVERVIEW

This chapter presents findings evaluating the internal structure of specimens prepared with the SGC and compares those results to specimens compacted with impact hammer. The comparison was performed using X-ray Computed Tomography (X-ray CT). Researchers also performed the Aggregate Image Measurement System (AIMS) test to characterize the physical properties of aggregate particles in specimens compacted with the SGC and impact hammer. To accomplish the works, researchers performed the following activities:

- Performed X-ray CT scans of the base and soil samples prepared using different compaction methods (SGC and impact hammer).
- Analyzed and interpret the data from X-ray CT scanning to quantify the air void distribution with depth (porosity gradients) for the different compaction methods.
- Performed the AIMS test to evaluate changes of physical aggregate properties (angularity, texture, and sphericity) after compaction with SGC and impact hammer.

X-RAY CT SCANNING

To examine nondestructively the internal structure of specimens compacted with the SGC and impact hammer, researchers performed the X-ray CT scan on three flex base and one subgrade soil material with the help of the Chevron Petrophysical Imaging Laboratory in the Department of Petroleum Engineering at the Texas A&M University.

Overview of X-Ray CT Scanner

The Chevron Petrophysical Imaging Laboratory is equipped with a state-of-the-art Toshiba Aquilion^{TM} RXL CT Scanner (Figure 20). The technology is used to produce cross-sectional (tomographic) images of a compacted specimen, allowing users to see inside the sample nondestructively and to determine air void and density gradients by advanced data processing techniques. The tomographic images were collected every 0.3 mm throughout the specimen height.
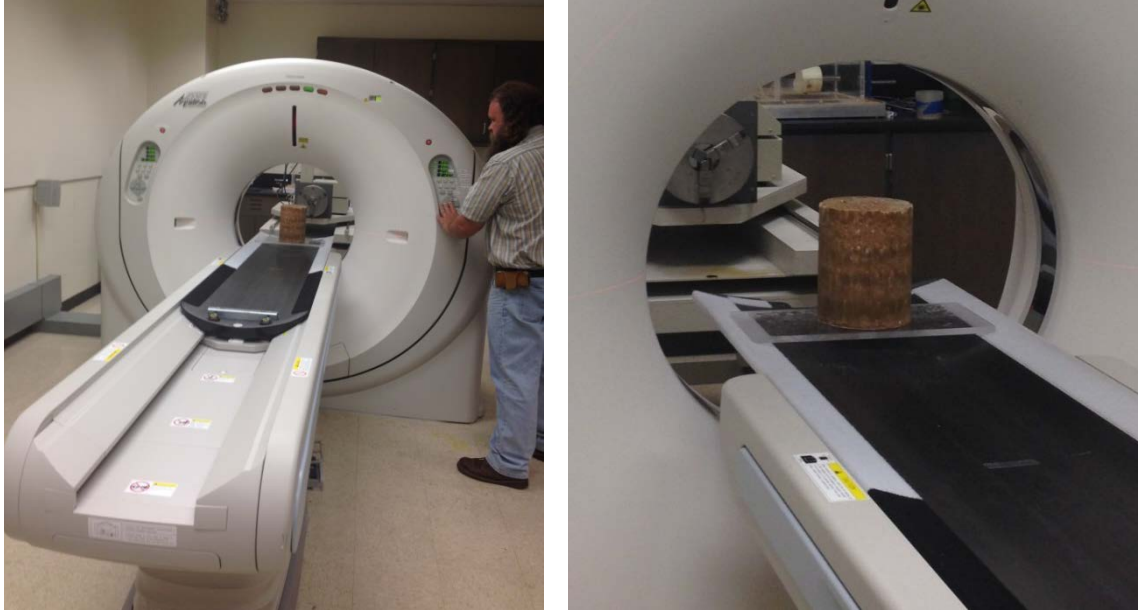
Figure 20. X-Ray CT Scanning of Compacted Sample.

X-Ray CT Scan Results

Using the tomographic images collected from the X-ray CT scanning, the percent air voids with depth (porosity gradient) of each specimen was determined.

Subgrade Soil material

Figure 21 shows the X-ray CT results of the Paris subgrade soil samples, including the CT images and corresponding air void distributions of specimens compacted with the SGC and impact hammer. As shown in Figure 21, the specimen compacted with impact hammer shows clear interfaces between lifts and air void gradients within each lift. The top of each lift has lower porosity, namely higher density, while the bottom has higher porosity. On the other hand, the air void distribution of the SGC sample indicates considerably more uniformity as compared to the impact hammer sample. The porosity gradient probably relates to the observed lower precision and repeatability of compressive strength test results on the subgrade soil samples compacted with the impact hammer.
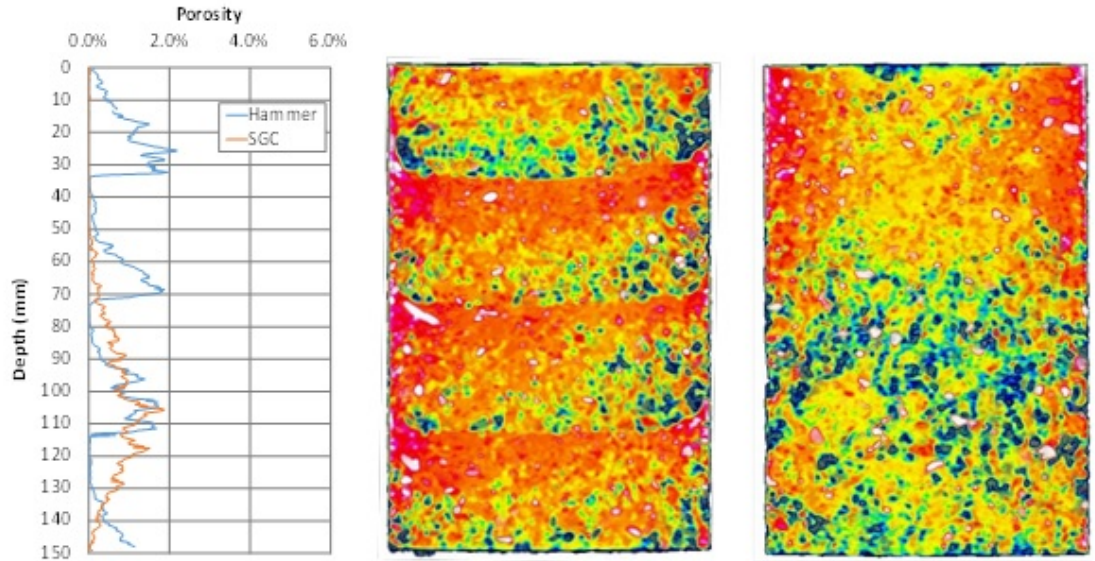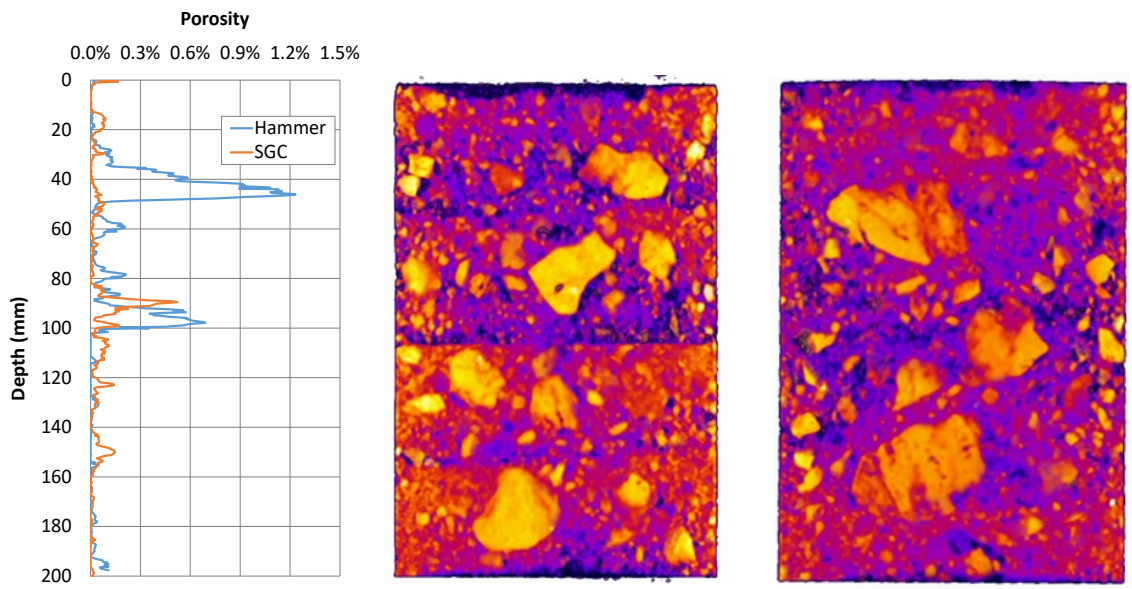
(a) Porosity Gradient   (b) Impact Hammer Compaction   (c) SGC Compaction

Figure 21. X-Ray CT Scan of Paris Subgrade Soil.
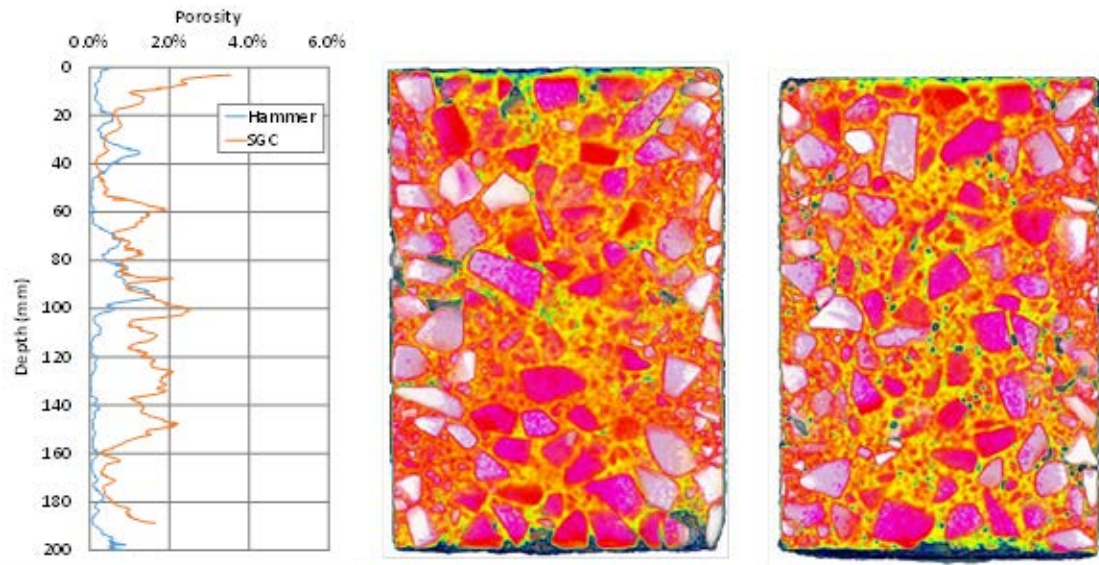
Flex Base Materials

Researchers performed the X-ray CT scanning test to characterize the internal structures in Pharr, San Antonio, and Waco base materials compacted with the SGC and impact hammer. For the Pharr material shown in Figure 22, the specimen compacted with the impact hammer shows clear lift interfaces while the SGC specimen shows relatively uniform structure throughout the height. Accordingly, the impact hammer specimen exhibits porosity gradients even within each lift while the SGC specimen's porosity is fairly uniform as shown in Figure 22(a).

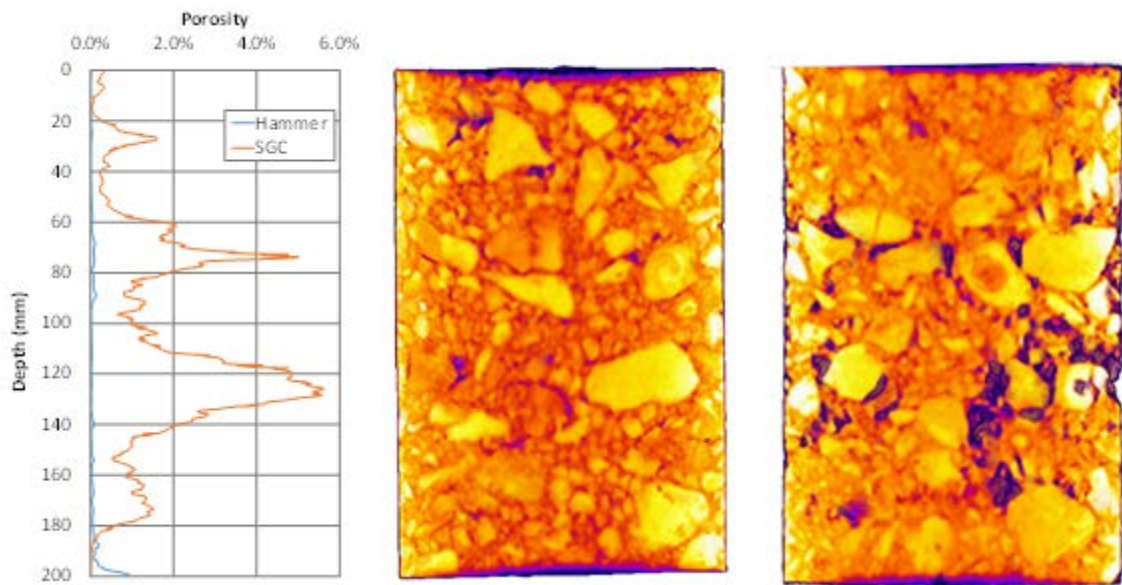**(a) Porosity Gradient   (b) Impact Hammer Compaction   (c) SGC Compaction**

Figure 22. X-Ray CT Scan of Pharr Base Material.

For the San Antonio and Waco base materials, the X-ray CT scan results exhibit a contradictory nature to the results from the Pharr base material. The Pharr sample compacted with the impact hammer showed higher air void and non-uniform distribution throughout specimens as compared to the SGC compaction. However, for San Antonio and Waco base materials, the air void distributions from SGC-compacted samples are less-uniform, particularly at the middle of sample, as shown in Figure 23 and Figure 24. Also, there is no clear interface between lifts at the impact hammer samples as found in the Pharr base material.

(a) Porosity Gradient   (b) Impact Hammer Compaction   (c) SGC Compaction

Figure 23. X-Ray CT Scan of San Antonio Base Material.

(a) Porosity Gradient   (b) Impact Hammer Compaction   (c) SGC Compaction

Figure 24. X-Ray CT Scan of Waco Base Material.

To explore the contradictory nature of the X-ray CT results, researchers performed gradation analysis using wet sieving. Figure 25 illustrates the gradation curves for the three base materials. Figure 25 shows the Pharr base material is fine grained aggregate while the San Antonio and Waco materials have coarser grained particles. Based on the gradation analysis and X-ray CT scan test results, researchers believes that the higher porosity variability within the San Antonio and Waco samples compacted with SGC is due to the course particle size distribution, which affects interlocking behavior of soil particles during the SGC compaction. Also, the coarse aggregate particles will make it harder for the SGC compaction energy to reach the middle of the sample, causing higher porosity at the middle of samples. Further study should be performed to investigate the SGC compaction energy and particle interlocking behaviors during the compaction.
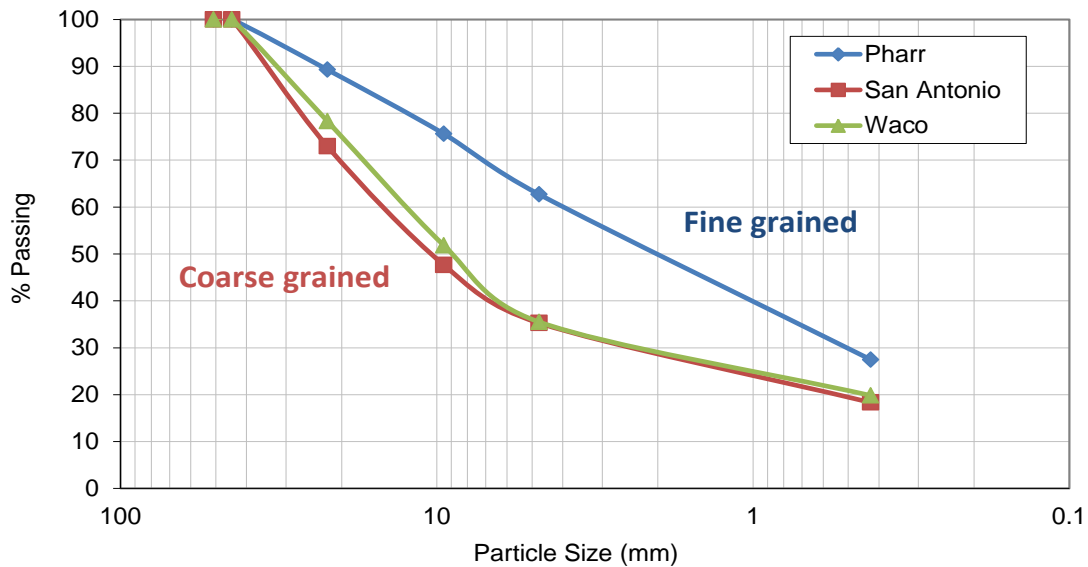

Figure 25. Particle Size Distribution Curves.

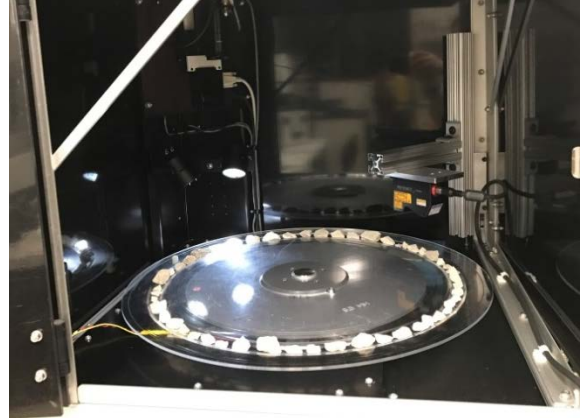## AGGREGATE IMAGE MEASUREMENT SYSTEM TEST

The physical aggregate properties such as angularity, surface texture, and sphericity have been shown to directly affect the engineering properties of base materials (*18*, *19*). To measure those aggregate properties, researchers performed the AIMS test.

Overview of AIMS Test

The AIMS is an integrated system consisting of image acquisition hardware and a computer to run the system and analyze data, as illustrated in Figure 26 (*18*). While the system provides a separate measurement function for fine or course particles, this study accounted for only course aggregate properties since the course particles seem to play an important role in internal structure of specimens prepared with the SGC and impact hammer. To measure potential aggregate property changes influenced by compaction methods, researchers measured the angularity, surface texture, and sphericity before compaction and after SGC and impact hammer compaction. Researchers also interpreted the results to help explain and correlate the results with the resilient modulus and permanent deformation behavior of each base material.
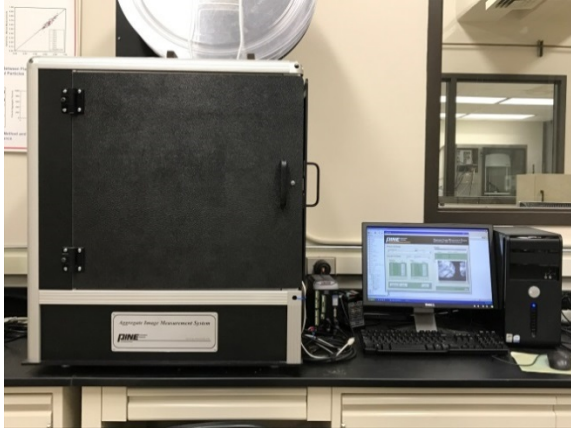
(a) AIMS Setup   (b) Sample Distribution Tray

Figure 26. Aggregate Image Measurement System.

AIMS Test Results

To measure the angularity, surface texture, and sphericity of the base materials, researchers performed the AIMS test for the following coarse aggregate particle sizes (Figure 27):

- Passing 1¾ in. and retained on 7/8 in. sieve.
- Passing 7/8 in. and retained on 3/8 in. sieve.
- Passing 3/8 in. and retained on #4 sieve.

**Figure 27. Aggregate Particles Used for AIMS Test.**

Angularity

The angularity describes variation at the particle boundary that influences the overall shape. It is analyzed by quantifying the change in the gradient on a particle boundary and is related to the sharpness of the corners of 2-dimensional images of aggregate particles (*18*). The angularity has a relative scale of 0 to 10,000 with a perfect circle having a value of 0. Figure 28 shows the angularity changes of three different particle sizes by compaction methods. These data indicate:

- For the largest aggregate particles retained on 7/8 in. sieve (Figure 28(a)), compacting samples makes the particles have more angular shape and sharper edges. Moreover,

specimens compacted with SGC show more increases in angularity than specimens compacted with the impact hammer, except for the Pharr material.
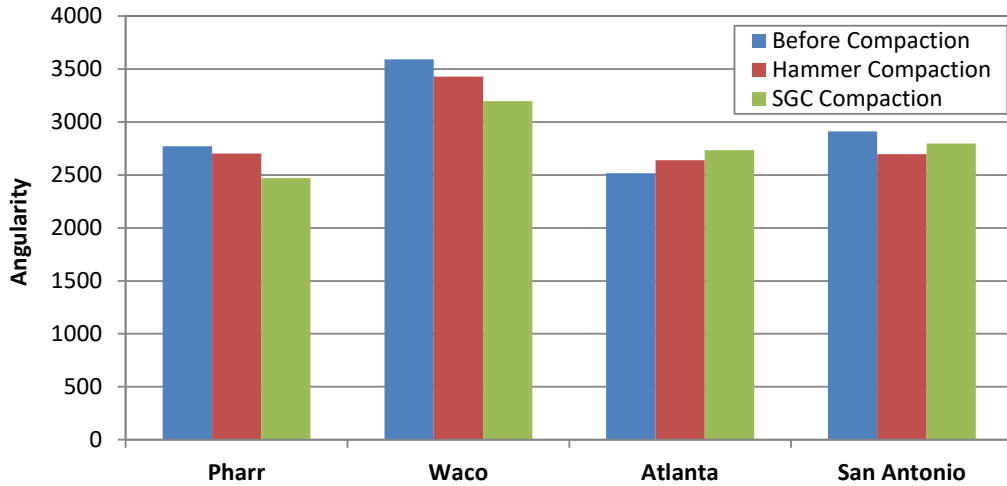
- For aggregate particles retained on 3/8 in. and retained on the No. 4 sieve, the data do not show an evident feature in angularity changes by compaction methods.
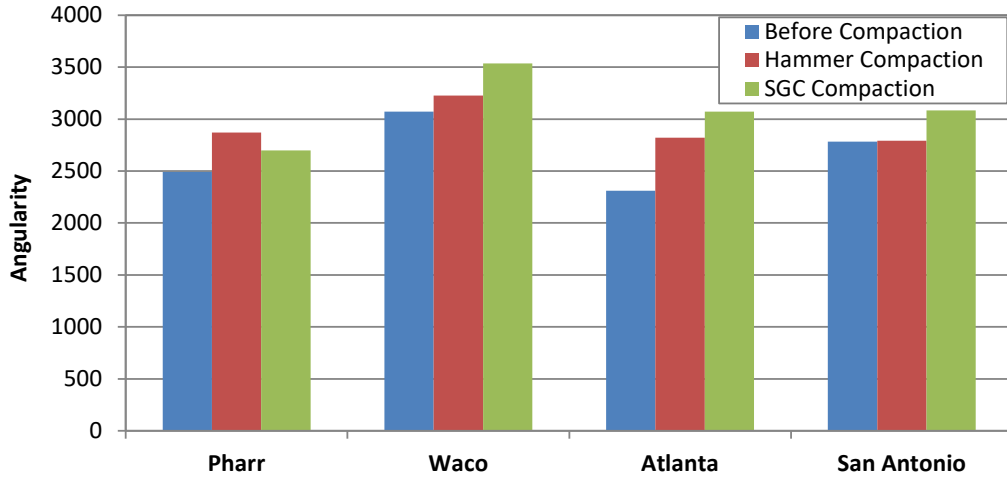
(a) Aggregate Retained on 7/8 in. Sieve
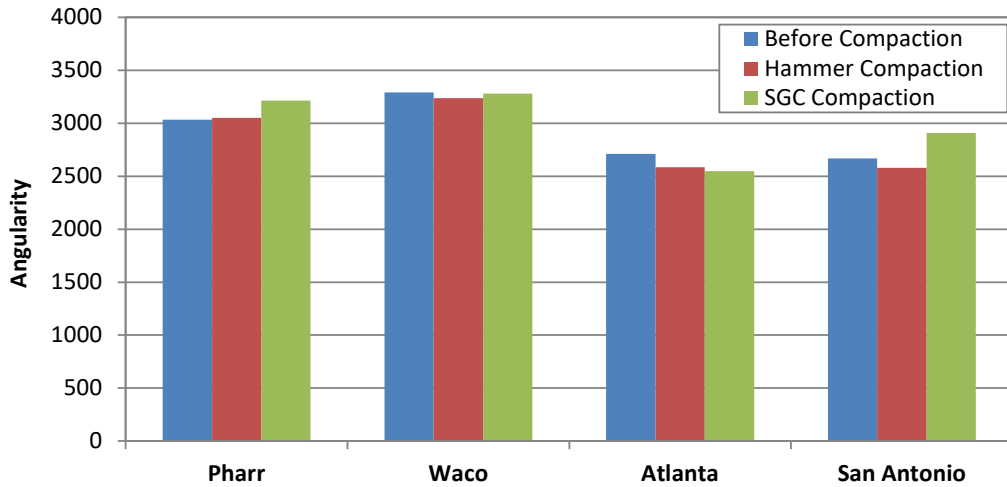
(b) Aggregate Retained on 3/8 in. Sieve

(c) Aggregate Retained on No. 4 Sieve

Figure 28. AIMS Angularity of Coarse Aggregates.

Surface Texture

The AIMS surface texture describes the relative smoothness or roughness of aggregate particles' surface micro-texture (less than approximately 0.5 mm in size), which is too small to affect the overall shape. The texture has a relative scale of 0 to 1000 with a smooth polished surface approaching a value of 0. As shown in Figure 29, the data do not show any evident feature or correlation between the surface texture and compaction methods.
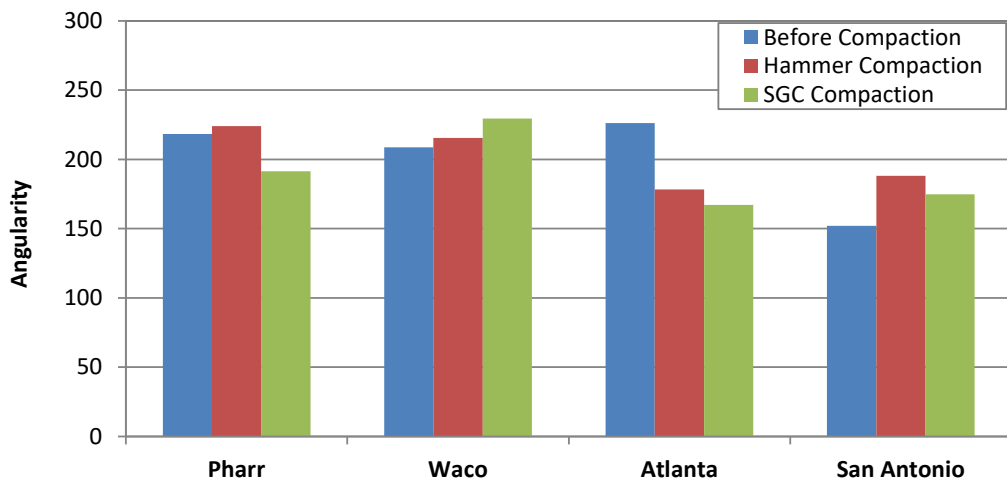
(a) Aggregate Retained on 7/8 in. Sieve

(b) Aggregate Retained on 3/8 in. Sieve

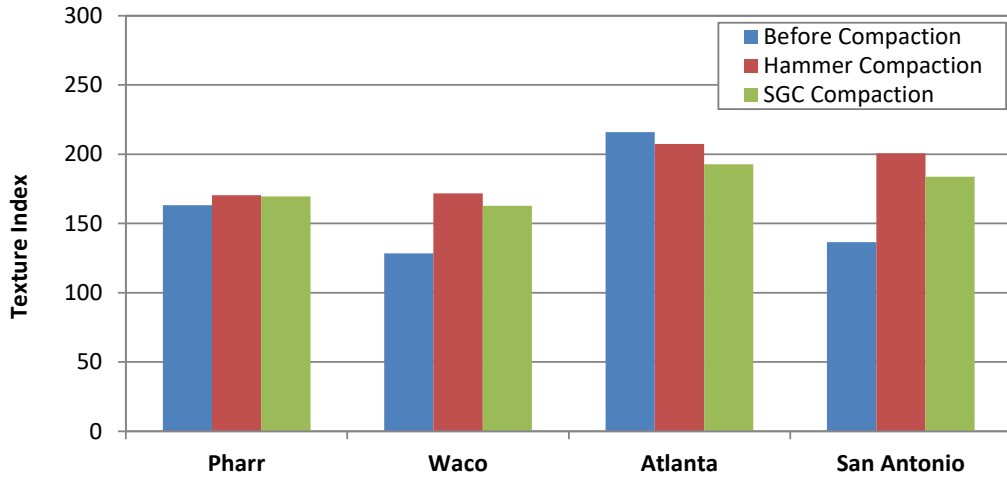**(c) Aggregate Retained on No. 4 Sieve**
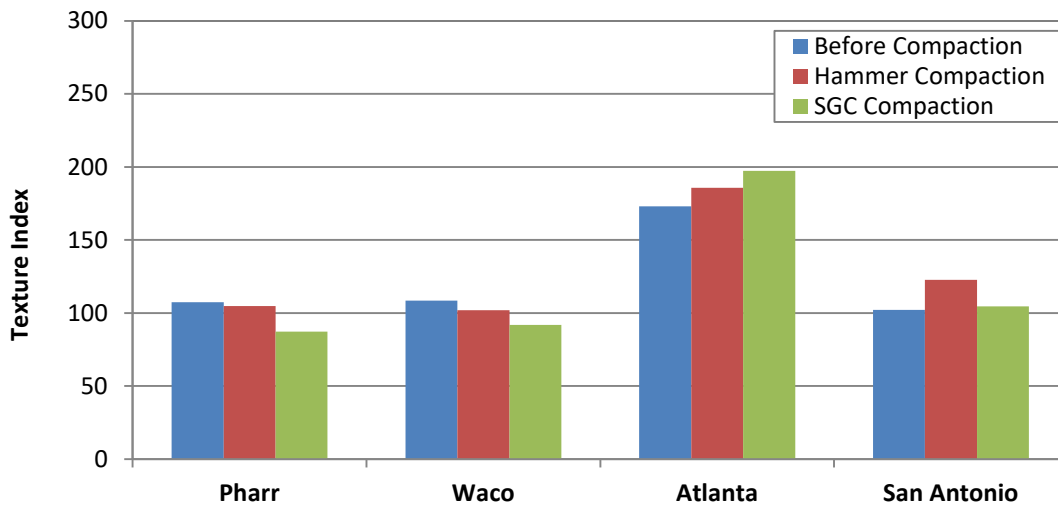
Figure 29. AIMS Texture of Coarse Aggregates.

Sphericity

Sphericity applies to coarse aggregate sizes and describes the overall 3-dimensional shape of a particle calculated with Equation 5.1. The relative scale of sphericity is 0 to 1 that one indicates a particle has equal dimensions (cubical).

$$\text{Sphericity} = \sqrt[3]{\frac{d_s d_I}{d_L^2}}$$ (5.1)

where d_s, d_I, and d_L^2 are particle shortest, intermediate, and longest dimensions, respectively. Figure 30 shows the sphericity of different particle sizes and compaction methods, and these data indicate:

- For the largest aggregate particles retained on 7/8 in. sieve (Figure 30(a)), compacting samples makes the particles more spherical or cubical. Moreover, specimens compacted with the SGC show slightly more increase in sphericity than specimens compacted with impact hammer. However, the Waco material indicates slightly different results from the other base materials tested.
- For aggregate particles retained on 3/8 in. and No. 4 sieve, the data do not show an evident feature in sphericity changes by compaction method.

(a) Aggregate Retained on 7/8 in. Sieve
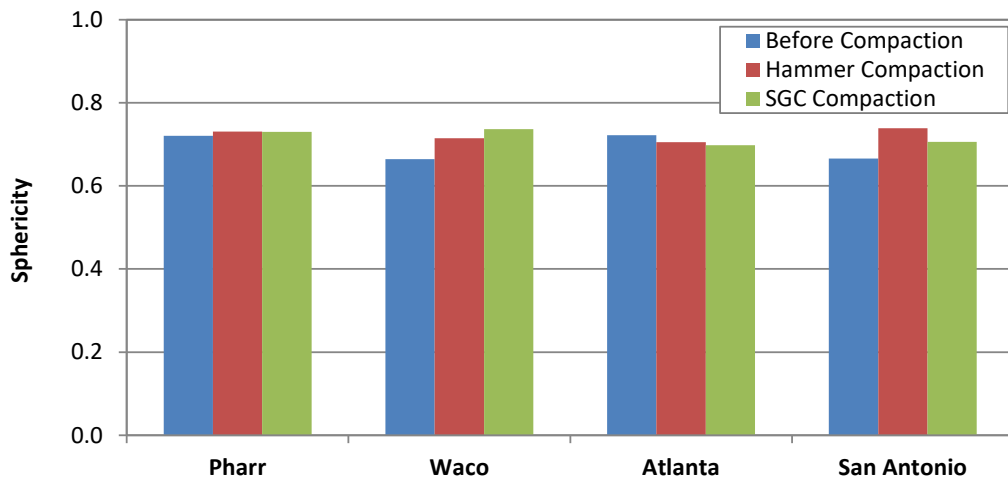
(b) Aggregate Retained on 3/8 in. Sieve
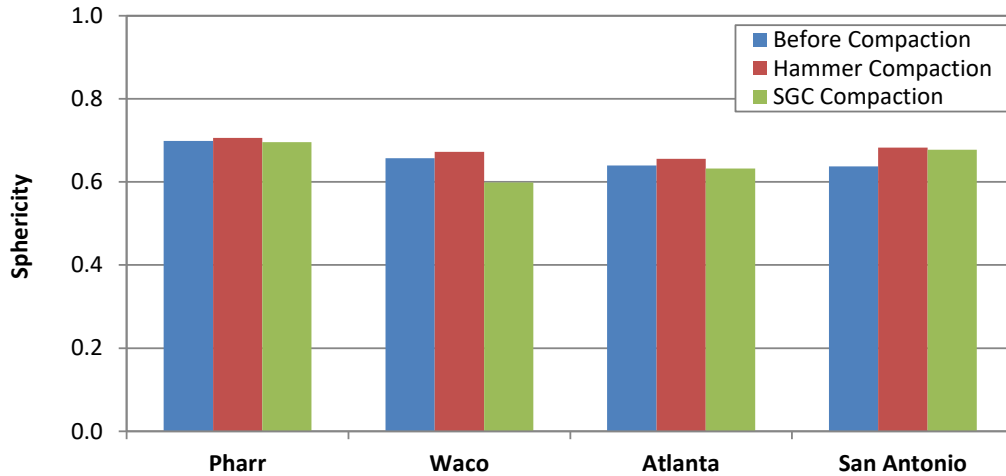
(c) Aggregate Retained on No. 4 Sieve
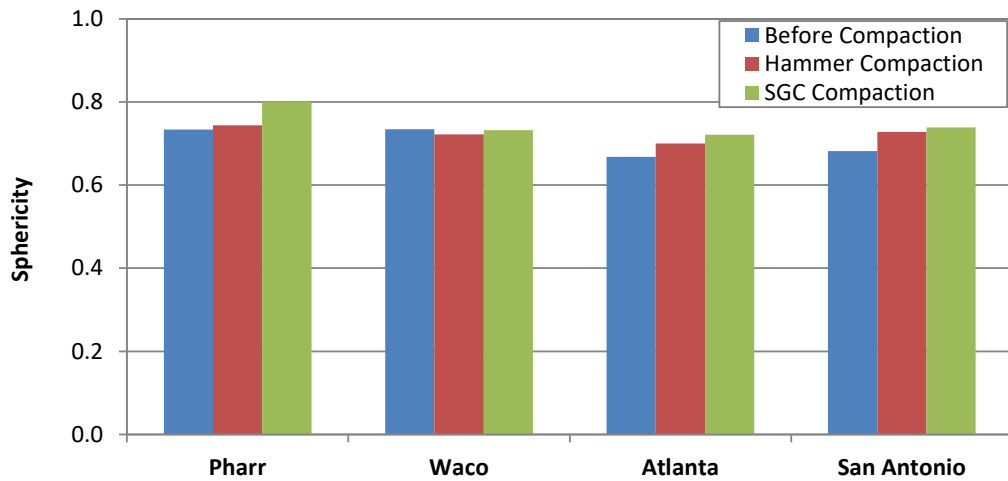
Figure 30. AIMS Sphericity of Coarse Aggregates.

Based on the impact of compaction method on angularity and sphericity, Figure 31 illustrates a possible mechanism explaining observed differences in performance test results. The data show:

- Pharr base material: SGC compaction increased sphericity, reduced angularity, and resulted in lower resilient modulus and increased permanent deformation.
- Waco, Atlanta, and San Antonio base materials: SGC compaction had minimal effect on sphericity, but increased angularity, resulting in increased resilient modulus and reduced permanent deformation.

These findings agree with the literature, which show that aggregates with more angular particles have better resistance to permanent deformation and generally increased resilient modulus due to better particle interlock and higher angle of shear resistance between particles (*19*, *20*, *21*).

To explore the contradictory nature of the Pharr material results on the shape change by the compaction methods, researchers re-evaluated the base material gradations illustrated in Figure 25. The gradation shows that only the Pharr material is fine-grained, while the other base materials are coarse-grained. Based on the gradation analysis and AIMS test, the data suggest that the fine-grained matrix within the Pharr material covers and protects the large aggregate particles from becoming more angular during the kneading action of SGC, which reduces particle interlock and angle of shear resistance between particles and results in the observed increases in permanent strain. In contrast, the coarse-grain gradation of the other materials results in increased contact areas between the course aggregate particles and makes the particles become more angular during the SGC kneading action, which results in higher resistance to permanent deformation.
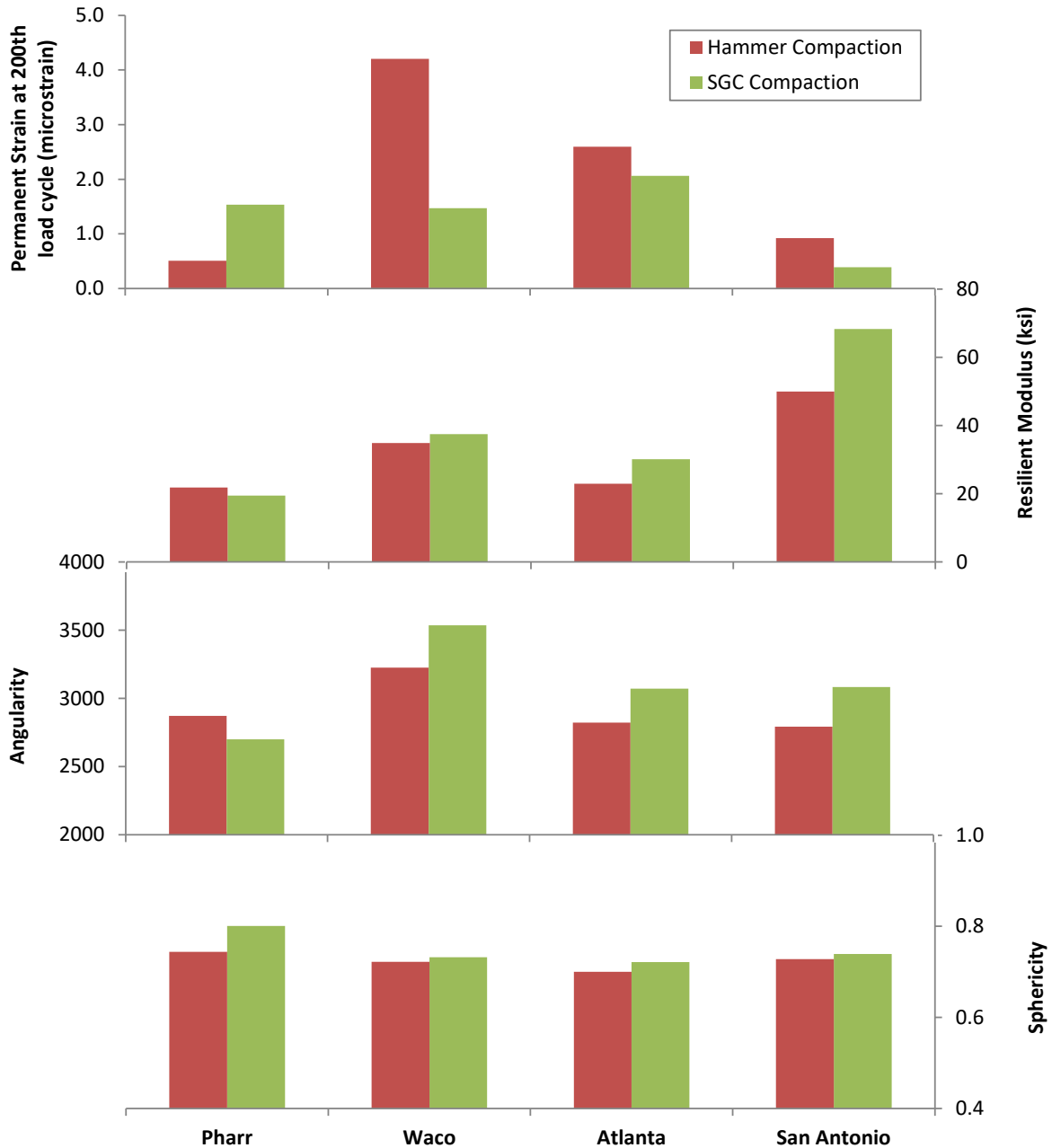
Figure 31. Comparisons between Performance Tests and AIMS Test Results.

SUMMARY

The major findings from the internal structure evaluation of materials using the X-ray CT scan and AIMS are summarized as follows:

- Researchers performed the X-ray CT scan tests and determined the percent air voids (porosity) with depth of each specimen:
  - For the Paris subgrade soil material, the samples compacted with SGC showed uniform air void distribution with depth with lower porosity while the impact hammer samples exhibited clear interface layers between lifts and porosity

54

gradient in each lift. The variability in porosity gradient from impact hammer compaction results in lower precision and repeatability of compressive strength test as compared to the SGC compaction.

- o For the base materials, the Pharr material showed fairly uniform structure and air void distribution in the SGC samples while the San Antonio and Waco base materials exhibited a contradictory nature to the Pharr material. For the San Antonio and Waco base materials, the air void distributions of samples compacted with SGC were more variable. Also, for the San Antonio and Waco base materials no clear interface was observed between lifts in the samples compacted with the impact hammer.
- o The contradictory nature of X-ray CT results from the materials may be due to the coarse particle size distribution of the San Antonio and Waco base materials, which affects interlocking behavior of particles during the SGC compaction.

- The AIMS test evaluated the changes of physical aggregate properties including angularity, texture, and sphericity, after the impact hammer and SGC compaction:
    - o For angularity, compacting samples made the particles have more angular shape and sharper edges for the particles retained on the 7/8 in. sieve. The samples compacted with SGC showed more increases in angularity than samples compacted with the impact hammer, except for the Pharr material. The data did not show an evident impact of compaction method on the angularity of 3/8 in. and No. 4 size particles.
    - o For the surface texture, the data did not show any evident feature or correlation with the compaction methods.
    - o The sphericity property showed similar results as angularity. Samples compacted with SGC were slightly more spherical or cubical as compared to impact hammer for the particles retained on the 7/8 in. sieve. However, the data did not show any evident feature in sphericity changes by compaction method for 3/8 in. and No. 4 sieve particle sizes.
    - o In context with resilient modulus and permanent deformation performance tests, the AIMS results show samples compacted with SGC generally had significantly higher angularity and slightly increased sphericity, where the angularity effect dominated and resulted in higher rutting resistance and increased resilient modulus as compared to specimens prepared with the impact hammer.

CHAPTER 6. SUMMARY AND CONCLUSIONS

This project explored the use of SGC to investigate if the gyratory compaction enables improved precision of compressive strength tests for flexible base and subgrade materials. The project also explored developing a procedure for determining the moisture-density curve of base and subgrade materials using the SGC. Also, the applicability of SGC for the materials was evaluated in context of M-E pavement design methods. These objectives were accomplished through extensive laboratory testing using four base materials and one subgrade soil with an emphasis on improving the precision of laboratory compaction and strength tests. The works for comparing the compressive strengths from the impact hammer and SGC compactions support the following conclusions:

- While the materials compacted with the SGC showed slightly lower compressive strength than materials compacted with the impact hammer, the statistical analysis indicated that the averaged strength test results from the SGC compaction are generally not statistically different with the test results from the impact hammer compaction.
- The SGC compaction generated the compressive strength results with less variability and improved precision compared to the impact hammer compaction.
- Given the improved precision of UCS results from SGC compaction, the draft procedure in the Appendix should be considered an alternate method for preparing flexible base specimens for strength testing.

The examination of the use of SGC in generation of moisture-density curves showed that the SGC compaction for base materials produced slightly higher OMC and MDD compared to the impact hammer compaction. However, for the subgrade soil, the OMC from SGC compaction is higher than one of impact hammer while the MDD from SGC compaction is lower. This discrepancy might be the result of different compaction mechanisms between gyratory compaction and impact hammer.

From the measurement of M-E design properties through the repeated load triaxial testing, the following findings and conclusions were drawn:

- The base materials compacted with the SGC were associated with lower accumulated permanent strains than ones compacted with the impact hammer.
- Similar to result of the permanent deformation behavior, the resilient modulus measured using the samples compacted with the SGC was higher than one with the impact hammer.
- From the results, the M-E design properties are not unique soil characteristics but may depend on the compaction method, where the compaction process can result in changes in aggregate shape properties and thus influence the M-E design properties.

The internal structure and aggregate particle shapes of specimens prepared with the SGC and impact hammer were investigated using X-ray CT and AIMS, respectively. The investigation suggested meaningful aspects from SGC compaction as follows:

- For subgrade and fine-grained base materials, the samples compacted with SGC showed uniform air void distribution with depth with lower porosity while the impact hammer samples exhibited clear interface layers between lifts and porosity gradient in each lift.

- For coarse-grained base materials, the air void distributions of samples compacted with SGC were more variable while no clear interface was observed between lifts in the samples compacted with the impact hammer.
- The higher porosity variability within samples compacted with SGC may be due to the course particle size distribution, which affects interlocking behavior of soil particles during the SGC compaction. Also, the coarse aggregate particles make it harder for the SGC compaction energy to reach the middle of the sample, causing higher porosity at the middle of samples.
- The AIMS results showed that the samples compacted with the SGC generally had higher angularity and slightly increased sphericity, where the angularity effect dominated and resulted in lower permanent strains and higher resilient modulus as compared to specimens compacted with the impact hammer.

In conclusion, the SGC compaction can offer an alternative lab method for constructing flexible base test specimens with improved precision in compressive strength. Improvement in compressive strength precision would reduce risk to both TxDOT and producers. The SGC compaction may also be used for establishing the OMC and MDD. However, as compared to using impact hammer for establishing the OMC and MDD, using the SGC to establish the moisture-density relationship would likely result in slightly different field compaction targets. For the M-E design, the SGC compaction method should be considered a possible factor that influences results in the development of M-E inputs from laboratory testing.

REFERENCES

1 Kim, W., Labuz, J. F., and Shongtao, D. "Resilient Modulus of Base Course Containing Recycled Asphalt Pavement," *Journal of Transportation Research Board*, 2007.

2 Fenwick, W. "Gyratory compaction of soil: report 3: crushed limestone, data report," US Army Engineer Waterways Experiment Station-Corps of Engineers, 1969.

3 Mokwa, R., Cuelho, E., and Browne, M. "Laboratory Testing of Soil Using the Superpave Gyratory Compactor" Presented at 87th Annual Meeting of the Transportation Research Board, Washington, D.C., 2008.

4 Ping, W. V., Michael Leonard, and Zenghai Yang. *Laboratory simulation of field compaction characteristics (Phase I).* No. FL/DOT/RMC/BB-890 (F), Florida A&M University-Florida State University College of Engineering, 2003.

5 Hossein, S. and Lane, S. *Development of a Catalog of Resilient Modulus Values for Aggregate Base for Use With the Mechanistic-Empirical Pavement Design Guide (MEPDG).* Virginia Center for Transportation Innovation and Research, 2015.

6 Coenen, A. R., Kutay, M. E., Sefidmazgi, N. R., and Bahia, H. U. "Aggregate structure characterisation of asphalt mixtures using two-dimensional image analysis." *Road Materials and Pavement Design*, Vol. 13, No. 3, 2012.

7 Dehghan B. A., Guddati, M. N., and Kim, Y. R. "An algorithm for virtual fabrication of air voids in asphalt concrete." *International Journal of Pavement Engineering*, Vol. 17, No. 3, 2016.

8 TxDOT Tex-241-F, Test Procedure for Compacting Bituminous Specimens using the Superpave Gyratory Compactor, Texas Department of Transportation, Austin, 2015.

9 AASHTO T 312-15, Standard Method of Test for Preparing and determining the density of Asphalt Mixture Specimens by Means of the Superpave Gyratory Compactor, AASHTO, Washington D.C., 2015.

10 ASTM D6925-15, Standard Test Method for Preparation and Determination of the Relative Density of Asphalt Mix Specimens by Means of the Superpave Gyratory Compactor, ASTM International, West Conshohocken, PA, 2015.

11 Huang, Y.H. *Pavement Analysis and Design*, 2nd ed. Prentice Hall, Inc., Upper Saddle River, NJ, 2004.

12 NCHRP, *Guide for Mechanistic-Empirical Design of New and Rehabilitated Pavement Structures*. NCHRP Project 1-37A, National Research Council, Washington, D.C., 2004.

13 Kenis, W. J. *Predictive design procedures, VESYS users manual: An interim design method for flexible pavements using the VESYS structural subsystem*. Final Report Federal Highway Administration, Washington, D.C., 1978.

14 Tseng K., and R. Lytton. "Prediction of permanent deformation in flexible pavement materials." In *Implication of aggregates in the design, construction, and performance of flexible pavements*. ASTM STP 1016, 1989, pp. 154–172.

15 Gu, F., H. Sahin, X. Luo, R. Luo, and R. L. Lytton. "Estimation of Resilient Modulus of Unbound Aggregates Using Performance-Related Base Course Properties," *ASCE Journal of Materials in Civil Engineering*, Vol. 27, No. 6, 2014.

16 NCHRP, *Recommended Standard Method for Routine Resilient Modulus Testing of Unbound Granular Base/Subbase Materials and Subgrade Soils.* NCHRP Protocol 1-28A. TRB, National Research Council, Washington, D.C., 2004.

17 Christopher, B. R., Schwartz, C., and Boudreau, R. *Geotechnical aspects of pavements*. US Department of Transportation publication No. FHWA NHI-05-037, 2006.

18 Pine Instrument, *Aggregate Image Measurement System Manual*, Pine Instrument Company, Grove City, PA, 2009.

19 Barksdale, R.D. and S.Y. Itani, "Influence of Aggregate Shape on Base Behavior," *Transportation Research Record 1227*, Transportation Research Board, National Research Council, Washington, D.C., 1989, pp 173–182.

20 Allen, J., *The Effect of Non-constant Lateral Pressures of the Resilient Response of Granular Materials*, Ph.D. Thesis, University of Illinois at Urbana-Champaign, 1973.

21 Rao, C., E. Tutumluer, and I.T. Kim, "Quantification of Coarse Aggregate Angularity based on Image Analysis," *Transportation Research Record 1787*, Transportation Research Board, National Research Council, Washington, D.C., 2002, pp 117–124.

APPENDIX. DRAFT TEST PROCEDURE FOR SUPERPAVE GYRATORY COMPACTION OF STRENGTH TEST SPECIMENS FOR SOILS AND BASE MATERIALS

Test Procedure for

SUPERPAVE GYRATORY COMPACTION OF STRENGTH TEST SPECIMENS FOR SOILS AND BASE MATERIALS

TxDOT Designation: Tex-XXX-X

Effective Date: XXX 2017

1	**SCOPE**

1.1   This method is used to compact cylindrical strength test specimens of soils and/or base (soil-aggregate mixture) materials using the Superpave gyratory compactor.

1.2   The values given in parentheses (if provided) are not standard and may not be exact mathematical conversions. Use each system of units separately. Combining values from the two systems may result in nonconformance with the standard.

2	**APPARATUS**

2.1   *Apparatus* used in Tex-117-E.

2.2   *Superpave gyratory compactor (SGC)*, calibrated in accordance with Tex-241-F.

2.3   *SGC specimen mold*, with an inside diameter of 149.90–150.00 mm (5.9–5.912 in.) and at least 250 mm (10 in.) high for base material, and 99.90–100.00 mm (3.933–3.937 in.) and at least 250 mm (10 in.) high for soils.

3	**PROCEDURE**

3.1   Prepare all materials in accordance with Tex-101-E, Part II.

3.2   Determine the optimum water content and maximum dry density of the material in accordance with Tex-113-E for base material and Tex-114-E for subgrade, embankment, and backfill.

3.3   Using the maximum dry density determined in Section 3.2, calculate the mass of air-dried material required to mold specimens.

3.3.1   Each specimen should be 150 mm (5.912 in.) in diameter ± 1.575 mm (0.0621 in.) and 200 mm (7.874 in.) in height ± 6.25 mm (0.246 in.) for base material and 100 mm (3.937 in.) in diameter ± 0.39 mm (0.015 in.) and 150 mm (5.912 in.) in height ± 0.065 mm (0.0026 in.) for subgrade, embankment, and backfill.

3.4   Weigh six individual samples using the mass of material calculated in Section 3.3.

3.5 Calculate and weigh the moisture to add to each specimen using the optimum moisture content determined in Section 3.2.

3.6 Place the total sample in the mixing pan, mix thoroughly, and wet with all of the mixing water by sprinkling water.

3.7 Cover the mixture with a non-absorptive lid to prevent moisture evaporation and allow to stand for 18–24 hours for base material and at least 12 hours for subgrade, embankment, and backfill.

3.8 Prior to compaction, weigh the sample, replace evaporated water, and thoroughly mix to ensure even distribution of water throughout the sample. Scrape material off mixing tools and into pan.

3.9 Cover and allow the samples to stand 1–2 hours before molding.

3.10 Prepare the samples in the SGC mold.

3.10.1 Base material.

3.10.1.1 Separate the sample using a 7/8 in. (22.6 mm) sieve.

3.10.1.2 Divide the material passing and retained on 7/8 in. (22.6 mm) sieve into four equal, homogeneous portions into separate non-absorptive bowls.

3.10.1.3 Construct the layer.

3.10.1.3.1 Place a non-porous paper disc in the bottom of the mold.

3.10.1.3.2 Cover the bottom of the mold with approximately 1/4 in. of material passing the 7/8 in. sieve and level with a spatula.

3.10.1.3.3 Hand place all of the aggregate particles retained on the 7/8 in. (22.6 mm) sieve that are contained in one non-absorptive bowls, minimizing contact with the edges of the mold.

3.10.1.3.4 Use a scoop held slightly above the top of the mold to pour the remaining weighed portion of material passing the 7/8 in. (22.6 mm) sieve into the mold.

3.10.1.3.5 Use a spatula to move the material passing the 7/8 in. sieve around to fill voids between the aggregate particles retained on the 7/8 in. sieve and cavities around the inside perimeter of the mold.

3.10.1.3.6 Level the surface with the spatula.

3.10.1.3.7 Repeat Sections 3.10.1.3.3–3.10.1.3.6 for each of the remaining lifts. Use all material to mold the sample in one lift. The surface of the fourth lift should be as free as possible from large aggregate.

3.10.1.3.8 When the material extends above the SGC mold, carefully press the material into the mold by hand or a slide hammer.

3.10.1.3.9   After all the material is in the mold, level the material with a spatula and place another paper disk.

3.10.1.3.10 Compact each specimen in accordance with Tex-241-F, Sections 8.1.5–8.1.10 to a height of 200 mm (7.874 in.) ± 6.25 mm (0.246 in.).

> **Note 1**–If the specimen fails to reach the specified height after applying a maximum number of gyrations that the compactor can apply, stop the compaction and discard the material in the mold. Prepare a new sample by Section 3.4–3.10, set higher compaction pressure in increment of 100 kPa, and compact the sample.

3.10.2   Subgrade, embankment, and backfill materials.

3.10.2.1   Place a non-porous paper disc in the bottom of the mold.

3.10.2.2   Place all material into the mold in one lift.

3.10.2.3   When the material extends above the SGC mold, carefully press the material into the mold by hand or a slide hammer.

3.10.2.4   After all the material is in the mold, level the material with a spatula and place another paper disk.

3.10.2.5   Compact each specimen in accordance with Tex-241-F, Sections 8.1.5–8.1.10 to a height of 150 mm (5.912 in.) ± 0.065 mm (0.0026 in.).

> **Note 2**-If the specimen fails to reach the specified height after applying a maximum number of gyrations that the compactor can apply, stop the compaction and discard the material in the mold. Prepare a new sample by Section 3.4–3.10, set higher compaction pressure in increment of 100 kPa, and compact the sample.

3.11   Extrude the specimen from the mold after the compaction is complete.

3.12   Record the weight of the compacted specimens.

3.13   Immediately after recording the weights, enclose the specimens in triaxial cells, with porous stones on top and bottom and non-porous paper discs between the specimen and porous stones to prevent moisture from traveling from the specimen into the porous stone.

3.14   Allow specimens to set 24 ± 1 hr undisturbed at room temperature.

3.15   Determine the strength of each specimen in accordance with Tex-117-E Part II.